FACULTEIT INDUSTRIËLE INGENIEURSWETENSCHAPPEN

master in de industriële wetenschappen: chemie

Masterproef

In Situ Measurement of Percolation Threshold of Conductive Fillers and Integration into a Self-Healing Elastomer

Promotor :
dr. Rita DE WAELE

Promotor :
prof. dr. ir. WIM DEFERME
drs. ing. STEVEN NAGELS

Copromotor :
Prof. dr. TANJA JUNKERS

Gezamenlijke opleiding Universiteit Hasselt en KU Leuven

Jarne Machiels

Scriptie ingediend tot het behalen van de graad van master in de industriële wetenschappen: chemie

KU LEUVEN | universiteit ▶▶hasselt

KU LEUVEN | universiteit ▶▶hasselt

2016•2017
Faculteit Industriële ingenieurswetenschappen
master in de industriële wetenschappen: chemie

Masterproef
In Situ Measurement of Percolation Threshold of Conductive Fillers and Integration into a Self-Healing Elastomer

Promotor :
dr. Rita DE WAELE

Promotor :
prof. dr. ir. WIM DEFERME
drs. ing. STEVEN NAGELS

Copromotor :
Prof. dr. TANJA JUNKERS

Jarne Machiels
Scriptie ingediend tot het behalen van de graad van master in de industriële wetenschappen: chemie

universiteit hasselt | KU LEUVEN

Acknowledgements

Table of contents

List of tables

List of illustrations

Glossary

Ag-Cu flakes:	Silver coated copper flakes
Ag MP's:	Silver microparticles
Ag NW's:	Silver nanowires
DBP:	Dibuthylphthalate
DPTA:	Dipropylene triamine
CB:	Carbon black
CB & CNT's:	Mixture of carbon black nanopowder and carbon nanotubes
CNT's:	Carbon nanotubes
CoSPo:	Conductive Self-Healing Polymer
CRA:	Controlled release agent
E(GaIn):	Eutectic gallium-indium
gf:	Gram force (1 gf = 0,0098 Newton)
HDPE:	High density polyethylene
L/D:	Aspect ratio (length/diameter)
MWCNT's:	Multi-walled carbon nanotubes
NR:	Natural Rubber
PDMS:	Polydimethylsiloxane
PEDOT/PSS:	Poly(3,4-ethylenedioxythiophene) polystyrene sulfonate
PHEMA:	Poly(2-hydroxyethyl methacrylate)
PNAGA-PAMPS:	Poly(N-acryloyl glycinamide-co-2-acrylamide-2-methylpropanesulfonic)
PP:	Polypropylene
PS:	Polystyrene
PVA:	Polyvinyl alcohol
P(VDF-TrFE):	Poly(vinylidenefluoride-co-trifluoro-ethylene)
SWCNT's:	Single-walled carbon nanotubes
THF:	Tetrahydrofuran
TPU:	Thermoplastic polyurethane
UV:	Ultraviolet
vol%:	Volume percentage
wt%:	Weight percentage

Abstract

One of many research topics at IMO-IMOMEC (Diepenbeek, BE) is the optimization of the design of printed structures and read-out electronics for the construction of flexible tactile sensors. This research focusses principally on the development of stretchable conductors by blending conductive fillers with an elastomeric matrix and the determination of the percolation threshold. Unfortunately, cracks can arise in the conductor while stretching which results in a loss of conductivity. Due to this crack formation, it is necessary to synthesize a conductive matrix with good blending characteristics, a low electrical resistance and reliable elastic properties.

In this research project, the percolation threshold of 6 different conductive fillers was determined by gradually increasing the volume percentage in a PDMS-matrix. During this experiment, an in situ measuring tool quantified the blend resistance to find out the percolation threshold. In the second stage of the investigation, the formation of cracks was prevented by using a self-healing elastomeric matrix instead of a traditional elastomer.

The percolation experiments show that cylindrical particles have a lower percolation threshold than spherical particles. Moreover, the blend resistance of metal fillers is smaller than carbon-based particles. Finally, the integration of conductive fillers in the self-healing elastomeric matrix results in a printable ink by the addition of chloroform.

Samenvatting

Eén van de vele onderzoektopics binnen IMO-IMOMEC (Diepenbeek, BE) handelt over de optimalisatie van het design van printbare structuren en read-out elektronica om flexibele, tactiele sensoren te ontwerpen. De focus ligt hoofdzakelijk op de ontwikkeling van rekbare geleiders door geleidende partikels in een elastomeermatrix te mengen en de bijhorende percolatiegrens te definiëren. Echter kan het rekken van geleidende structuren breuken veroorzaken met een verhoging van de weerstand tot gevolg. Om deze scheurvorming te vermijden, is het noodzakelijk om een homogeen geleidende matrix te synthetiseren met een lage weerstand en betrouwbare rekeigenschappen.

De percolatiegrens van 6 verschillende geleidende partikels is bepaald door de volumefractie in een PDMS-matrix geleidelijk te verhogen. Tijdens dit experiment bepaalt een in-situ meetapparaat voortdurend de blendweerstand. In de tweede fase van het onderzoek is de elastomeermatrix vervangen door een zelf-herstellend elastomeer om scheurvorming te belemmeren.

De percolatie-experimenten tonen aan dat cilindrische partikels een lagere percolatiegrens vertonen dan sferische partikels. Uit dit experiment is ook de corresponderende blendweerstand bepaald, dewelke voor metalen partikels kleiner is dan voor koolstofhoudende partikels. Ten slotte resulteert de integratie van de geleidende partikels in het zelf-herstellend elastomeer in een printbare inkt door de toevoeging van chloroform.

Introduction

This master's thesis is performed at IMO-IMOMEC (Institute of Materials Research), a research institute of Hasselt University specialised in the development of innovative materials. Currently, IMO-IMOMEC is running an investigation to optimize the design in printed structures and read-out electronics to achieve property requirements for flexible tactile sensors. In addition, Hasselt University hopes to create in the near future a stretchable and printed electronic circuit that will be an important unit to design wearable electronics, robots, stretchable displays, flexible batteries and healthcare devices. These applications initially require the creation of stretchable electronic conductors and for that reason, IMO-IMOMEC focusses on its development by adjusting and studying the interaction between the geometry, the materials and the manufacturing methods.

Nowadays, literature already describes five distinctive manufacturing methods to create stretchable conductors. First of all, soft lithography can fabricate microchannels in elastomers. A conductive liquid-phase gallium-indium (GaIn) alloy fills these channels. Secondly, conductive particles can be implanted into the surface region of an elastomer. A third option is the infiltration of elastomers with conductive filler networks. Further, metal fillers can be synthesized within elastomers. The last possibility is a blend of conductive fillers with an elastomeric matrix [1], [2].

This master's thesis investigates the last option in more depth, namely mixing conductive fillers with a non-conductive elastomeric matrix. If the number of conductive particles is too low, the resistance of the blend is too high for electrical conductivity. On the other hand, a surplus of conductive fillers does not decrease significantly the minimal resistance and is not opportune due to the cost-price of the fillers. Ergo, it is essential to determine the volume percentage of the conductive fillers in the elastomeric matrix where the blend alters from insulator to conductor.

The first complication of this master's thesis is the measurement of the blend resistance. Generally, a sample is taken of the blend, poured into a mould and cured. Afterwards, the resistance is measured one time by a four-wire measurement, but it would be more interesting to measure in situ the resistance of the blend. In this master's thesis, an in situ measuring tool is designed by attaching tungsten electrodes in the bottom of a round bottom flask. It permanently quantifies the resistance of the blend with a four-wire measurement, meanwhile the results of the analysis are processed and saved with LabVIEW.

The second objective of this investigation is the determination of the percolation threshold of six different conductive fillers into a commercial elastomeric matrix. The percolation threshold is the transition of the elastomeric matrix from insulator to conductor observed with increasing fraction of conductive fillers. Carbon black (CB), multi-walled carbon nanotubes (MWCNT's), silver nanowires (Ag NW's), silver microparticles (Ag MP's), silver coated copper flakes (Ag-Cu flakes) and a mixture of carbon black nanopowder and carbon

nanotubes are separately blended with polydimethylsiloxane (PDMS), a high viscous polymer. The amount of conductive fillers in the PDMS-matrix is increased while the resistance of the blend is measured in situ. At a certain amount of conductive fillers, the conductivity of the blend rises quickly and the percolation threshold is accomplished. When the percolation threshold of each blend is determined, the optimal conductive filler and its concentration in the blend are selected by a trade-off between the desired resistance (max. 1 Ω) and the cost-price.

Another challenge is the possible occurrence of little cracks arising in the conductor while stretching. These cracks grow with each stretching and debilitate the conductor until overall fracture and loss of conductivity occurs. By using a self-healing elastomeric matrix, little cracks and damage are healed spontaneously without external aid. Ergo, the third objective of this master's thesis is the synthesis of a suitable self-healing elastomeric matrix with an extensibility of at least 100%, so that it can be stretched twice as long as originally.
This self-healing elastomer is synthesized from fatty acid derivatives, urea and dipropylene triamine (DPTA). By condensing DPTA with a mixture of fatty acid derivatives, randomly branched oligomers are obtained. In the second synthesis step, the oligomers react with urea to a self-healing elastomer [3].

The last objective of this master's thesis is to create a conductive self-healing elastomeric matrix by the integration of the optimal conductive fillers. After that, the viscosity of the conductive self-healing blend (ink) should be low enough in order to be processable by screen printing and/or blade coating. Finally, the extensibility and resistance are simultaneously measured while stretching the conductor. If the printed/coated conductor meets the requirements of conductivity and extensibility during this experiment and no cracks occur, the main goal of this master's thesis is accomplished.

1 Stretchable conductors

Stretchable electronic conductors have progressively generated interest, because of their enormous amount of possible applications. Soft robotics, malleable displays, wearable electronics, flexible batteries and healthcare devices (e.g. cardio stimulating and neuroprosthetic implant) demand flexible and conductive polymers, which can undergo large deformations without losing conductivity. Several research communities are trying to develop new manufacturing methods to create electronic conductors with a low electrical resistance and a high extensibility. Innovative material solutions are necessary to comply these specific requirements. Other interesting characteristics of this fast-growing research topic are the lightweight and the possible large-area printability [4], [5], [6], [7], [8].

The production of a material combining conductivity and extensibility remains a tremendous challenge. Due to the elongation of the chemical bonds during macroscale stretching, leading to delocalization of electronic orbitals, some defects can occur like the formation of cracks in the polymer or the increase of electrical resistance [8], [9]. The requirement of a stretchable conductor is to endure this operation without degradation in order that it is an interesting alternative for the existing rigid conductors. Due to their ability to deform, a stretchable conductor has a high mechanical reliability for stresses while a rigid conductor cannot resist the stresses and little cracks are formed [10].

The conductivity and extensibility of stretchable conductors are affected in three different ways. First of all, the geometry of the conductor can be adapted to create elasticity. Secondly, the used materials impress the flexibility of the conductor. Finally, the manufacturing method has a big influence on the extensibility of the conductor.

1.1 Geometry of the conductor

The geometry of an electronic conductor has an important hold on his properties, especially the extensibility. Different kinds of conductor designs are already observed: single line, zigzag, rectangular pulse, meander geometry and helical design. These designs are shown in Figure 1 [11], [12].
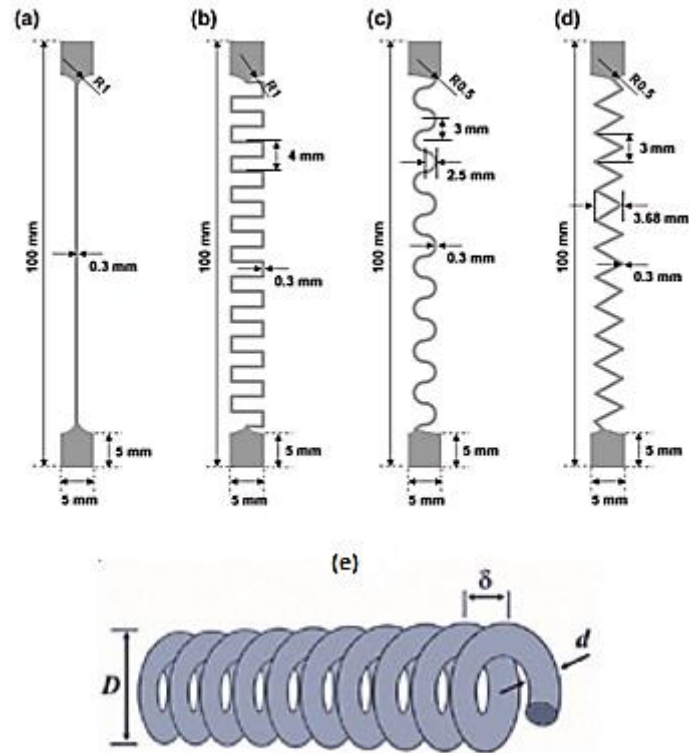
Figure 1: Different conductor designs: (a) single line, (b) rectangular pulse, (c) meander (horseshoe), (d) zigzag, (e) helical design [11], [12]

K.-S. Kim *et al.* investigated the influence of the conductor geometry on the extensibility and electrical resistance, using a monotonic tensile test. Figure 2 shows accurately the moment of failure of each conductor design as a quick rise of the electrical resistance. This increase is caused by the disconnection of conductive paths between the conductive fillers [11].
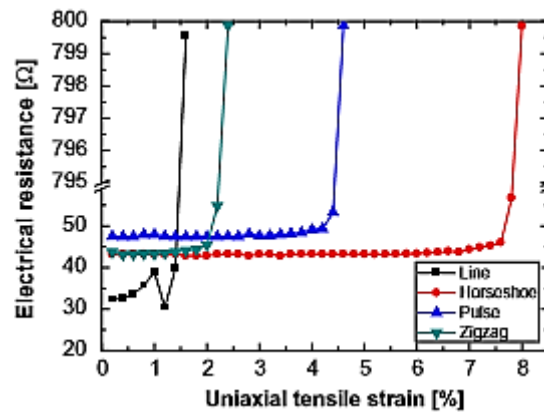
Figure 2: Electrical resistance as a function of tensile strain for various conductor designs [11]

The conclusion of this research is that the extensibility increases in the order of single line, zigzag, rectangular pulse and meander geometry. Due to this investigation, stretchable electronic conductors may preferably have a meander design.

18

Further research examined the effect of different meander shapes on the extensibility of an electronic conductor. Three different meander shapes – shown in Figure 3 – were investigated: the elliptical shape, the "U" shape and the horseshoe shape [13].
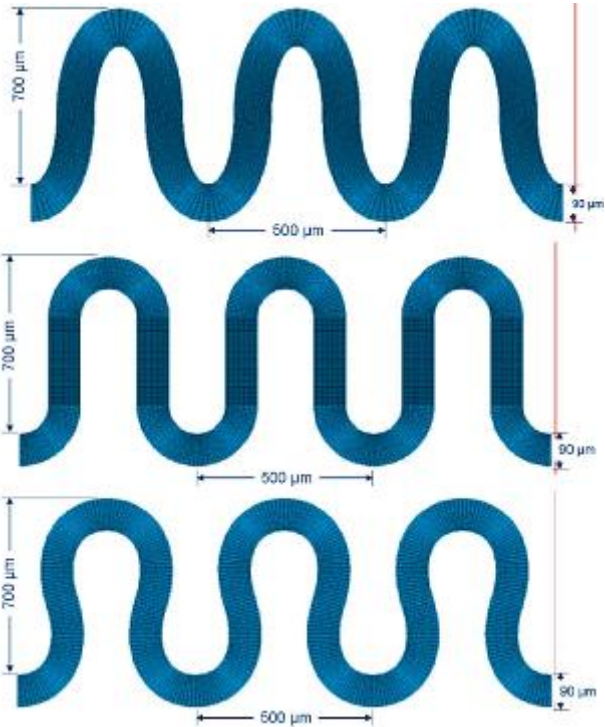
Figure 3: Different meander shapes: (top) elliptical shape, (middle) "U" shape, (down) horseshoe shape [13]

Gonzalez *et al.* applied a deformation of 20% in the axial direction of the meander. A high stress concentration was detected in the crest of the elliptical shape. This stress can be reduced by preferring a more round design, such as the "U" shape. In this case, there was a better stress distribution, but the reduced radius of curvature still limited it. In the horseshoe design, the stress was more distributed, especially in the extended part of the conductor. Figure 4 shows the stress distribution in the three different meander designs.
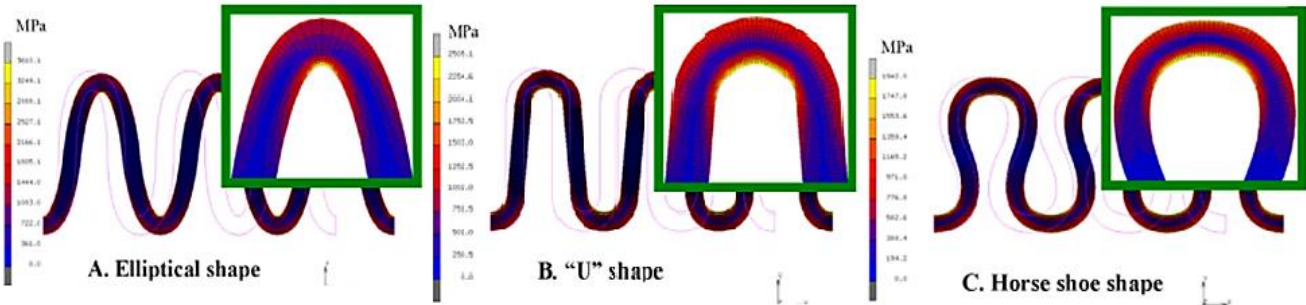
Figure 4: Stress distribution in three different conductor shapes: (a) elliptical shape, (b) "U" shape, (c) horseshoe shape [13]

More failures are expected in an elliptical shape than in a horseshoe shape, because cracks and failures generally appear in regions with a high stress concentration [13], [14].

The stresses in the conductor can even reduce more by subdividing the line (conductor) in several lines of smaller width. This multi-track horseshoe design, as shown in Figure 5, lowers the induced stress and increases the extensibility [13].
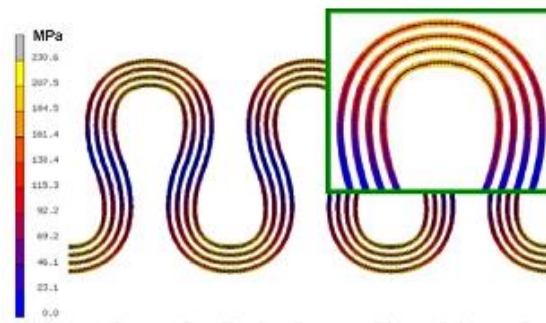
Figure 5: Stress distribution in a multi-track horseshoe [13]

The conclusion of this paragraph is that a multi-track horseshoe shape is the optimal conductor design for stretchable conductors.

1.2 Material of the conductor

The extensibility of an electronic conductor depends highly on the used materials. The conductor obtains elasticity by the employment of elastomeric materials. Currently, polydimethylsiloxane (PDMS) and thermoplastic polyurethane (TPU) are the most used elastomers. Though other polymers are also considered, like a paraffin wax-polyolefin thermoplastic blend [6], [7], [11].

On the other hand, the conductivity of the electronic conductor is caused by the use of conductive fillers. Possible conductive particles are carbon black (CB), carbon nanotubes (CNT's), copper particles, silver nanowires, silver microparticles, graphene… Some polymers can also cause conductivity, but their application is still limited [9], [15], [16].

A lot of combinations between elastomers and conductive fillers are conceivable. Due to this, researchers are still trying to figure out excellent combinations to increase extensibility and electrical conductivity.

1.3 Manufacturing methods of the conductor

The manufacturing method of a conductor (in combination with suitable materials) has a big influence on creating extensibility. Five distinctive methods to generate stretchable conductors are discussed: filling microchannels with liquid metals, implanting conductive fillers in elastomers, infiltrating elastomers with conductive filler networks, blending conductive fillers with elastic polymers and synthesizing metal fillers within elastomers [17].

1.3.1 Filling microchannels with liquid metals

This manufacturing method creates microfluidic channels in thin films of an elastomer, usually polydimethylsiloxane (PDMS), by soft lithography or using a CO_2 laser [1].

Soft lithography processes a wide range of elastomeric materials and refers to a collection of fabrication methods, all based on producing a patterned layer (Figure 6) of PDMS. Initially, a photosensitive layer covers the PDMS layer and is illuminated with UV-light. The patterned structure is obtained by a diversity of illumination. Unilluminated strips are removed from the layer and illuminated strips remain, resulting in a patterned layer.
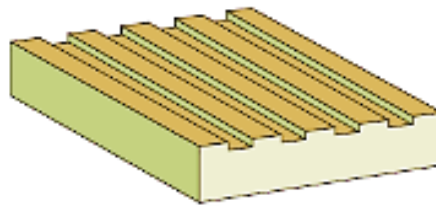
Figure 6: Patterned layer of PDMS by using soft lithography [18]

Further, the printed microchannels in the PDMS layer are closed with another layer of PDMS in order that they are properly sealed [17].

The next step is the introduction of liquid metals into the channels by using a syringe pump, as shown in Figure 7. Possible interesting metals are eutectic gallium-indium (EGaIn) alloy and gallium-indium-tin alloy, because they are molten at room temperature. Moreover, these alloys have an extreme extensibility without losing conductivity. Lastly, the liquid metal can repair little cracks or defects by reflowing through the channels [17].
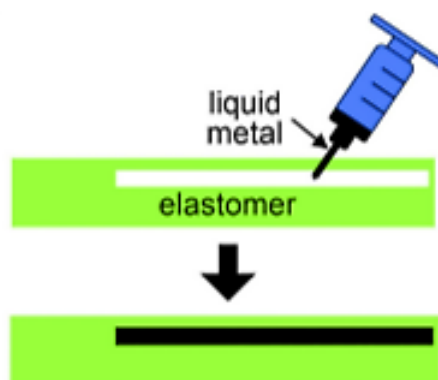
Figure 7: Schematic representation of filling microchannels with liquid metal [17]

This manufacturing method has also some disadvantages. Firstly, liquid metals are more expensive than copper or nickel. Furthermore, they can lose their extensibility at low temperatures, e.g. EGaIn is brittle at 0°C [17], [19].

1.3.2 Implanting conductive fillers in elastomers

The implantation of conductive fillers in elastomers is a second method of manufacturing stretchable conductors. In this case, conductive particles are directly embedded into the surface region of an elastomeric substrate, such as polydimethylsiloxane. This substrate is a chemical elastomer crosslinked by covalent bonds. Due to these crosslinks, the filler sources have to be accelerated to implant the conductive particles into the elastomer surface. Figure 8 shows the used technique, namely ion implantation. The surface properties are modified by doping them with ionic impurities, mostly metal cations. Due to the electrons of the polymer matrix, these doped cations reduce to metal atoms and aggregate into nanoparticles [17].
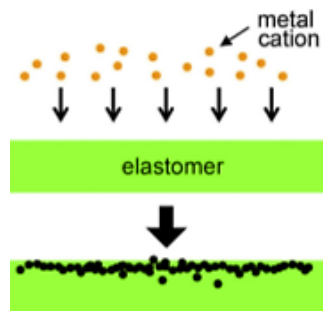
Figure 8: Schematic representation of implanting conductive fillers (metal cations) in an elastomer [17]

Another way to implant conductive fillers in elastomers is based on a printing technique. The PDMS substrate is stretched with a stretching apparatus. After that, the pre-stretched PDMS substrate is exposed to ultraviolet light. This illumination should modify the surface of the substrate, because PDMS is normally highly hydrophobic and not suitable for printing. Further, a conductive ink (e.g. silver ink) is printed or sprayed onto the pre-strained PDMS substrate. Finally, the substrate is annealed in a vacuum oven in order that there appears no cracks in the substrate. Figure 9 shows this method of implanting conductive fillers in elastomers with a printing technique [9], [20].
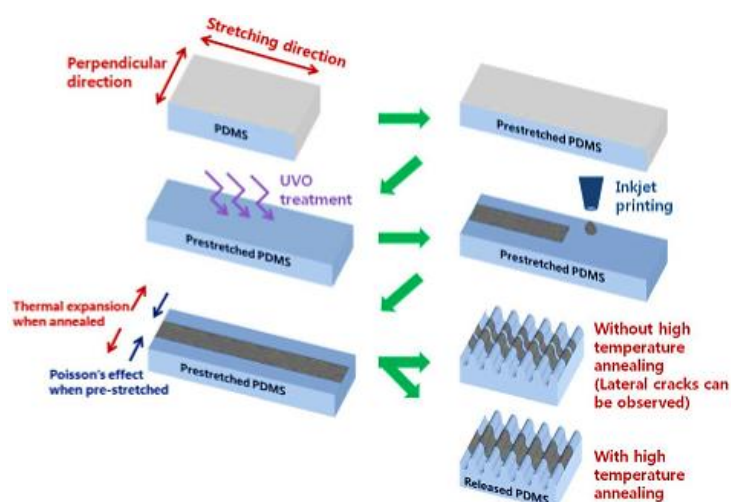
Figure 9: Printing a conductive film on a pre-stretched PDMS substrate [9]

22

1.3.3 Infiltrating elastomers with conductive fillers networks

This manufacturing method describes the infiltration of a thin film of conductive fillers in an elastomer by using a precleaned substrate. Figure 10 shows the main idea of this production technique.
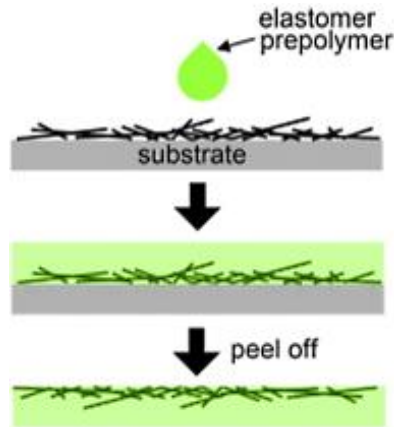
Figure 10: Schematic representation of infiltrating elastomers with conductive filler networks [17]

Initially, a suspension of conductive particles (e.g. single-walled carbon nanotubes) is sprayed onto the substrate, which could be a glass slide, a silicon wafer or plastic material. After that, the suspension is dried to form a conductive and uniform film of the conductive fillers. In the next step, liquid elastomer (e.g. PDMS) is sprayed over the surface of the conductive film, followed by curing. Finally, the substrate is peeled off and the conductive film is bound to the cured elastomeric layer. Due to this technique (Figure 11), a stretchable and highly conductive composite can be achieved [21], [22], [23].
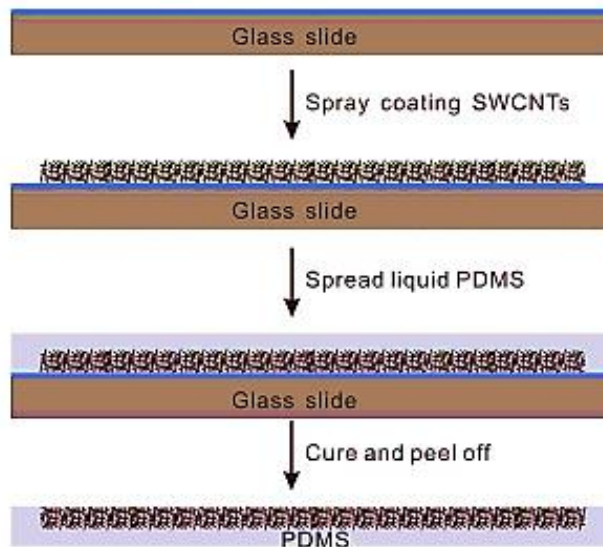
Figure 11: Schematic process of infiltrating silver nanowires in PDMS by using a silicon substrate [22]

1.3.4 Blending conductive fillers with elastic polymers

Another manufacturing method of stretchable conductors (as shown in Figure 12) is the mechanical blending of conductive fillers with an elastomeric matrix (e.g. PDMS). This technique is not effective for nanoparticles, because these particles aggregate fast in the polymer matrix during mixing. The mechanical homogenization is only suitable with microparticles (e.g. carbon nanotubes) where the kinetic energy of the microparticles can overcome the van der Waals attraction between the particles [17].
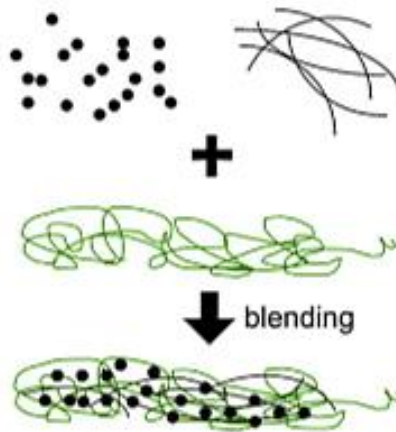
Figure 12: Schematic representation of blending conductive fillers with elastic polymers [17]

By increasing the volume percentage of conductive fillers, the conductivity of the blend rises quickly at a certain amount of conductive fillers and the percolation threshold is accomplished. The percolation threshold is the amount of conductive fillers where the elastomeric matrix transforms from insulator to conductor. At this point, there is a physical entanglement of conductive particles in the elastomeric matrix and a conductive blend is formed [24], [25].

1.3.5 Synthesizing metal fillers within elastomers

A last possibility to create stretchable conductors is the in situ synthesis of nanoparticles within elastomeric substrates, as shown in Figure 13. This process involves mixing a metal salt (metal precursor) in an elastomeric matrix or polymer gel and curing agent (hardener). During the curing process, the hardener has a dual role, namely crosslinking the elastomer and reducing the metal salt to nanoparticles.
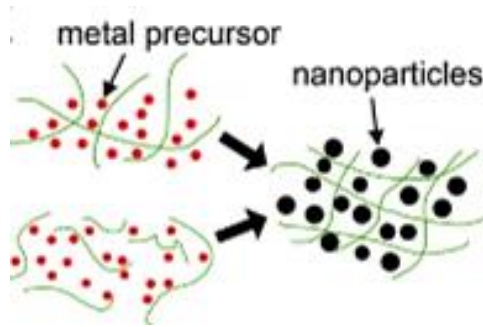
Figure 13: Schematic representation of synthesizing metal fillers within elastomers [17]

Chemical crosslinks are preferred over physical crosslinks, because they are mechanically stronger and better suitable for electronic devices. A thermal annealing or UV-exposure of the elastomeric matrix can induce these chemical crosslinks. Furthermore, the curing agent reduces the metal salt to form metal nanoparticles. This reduction only occurs by exposing the metal precursors to a reducing vapor or dipping in a reducing agent solution. The in situ synthesized nanoparticles do not even aggregate, because their movement is restricted by the elastomeric matrix. Finally, this synthesis method leads to a uniform dispersion of conductive nanoparticles in the elastomeric matrix [17], [26], [27].

2 Conductive blend

2.1 Introduction

The mechanical blending of conductive particles with an elastomeric matrix results in a conductive blend, suitable for the production of electrically conductive stretchable electronics. The added number of conductive fillers in the elastomeric matrix is an essential specification to generate conductivity. If the resistance of the blend is too high for electrical conductivity, the volume percentage of conductive particles should be increased. At a certain load of fillers, the resistance decreases quickly and the percolation threshold is achieved. On the other hand, an excess of conductive fillers does not alter the conductivity significantly. Moreover, a higher filler content leads to a higher viscosity and worse mechanical and rheological properties. Due to this and the high cost-price of the particles, it is not attractive to pass highly the percolation threshold.

A second important parameter of a conductive blend is the degree of dispersion of conductive fillers in the elastomeric matrix, which is dependent on the mixing time, stirring speed and viscosity of the blend. Extending the mixing time, optimising the stirring speed and decreasing the viscosity cause a better dispersion of particles in the blend [28], [29], [30].

Finally, the opportunity to scale up industrially the volume of a conductive blend is an enormous advantage. When the percolation threshold is known and the manufacturing process is optimised, the volume upscaling, that is dependent on the batch size, is quite simple to realize. Several machines are available to process the blend (ink) to an application, especially screen printers (e.g. see Figure 14) [31].

Figure 14: Screen printer with ventilation (IMO-IMOMEC)

2.2 Percolation theory

The connectivity of fillers within a polymer matrix and the result of this connectivity on the macroscale properties is described by the percolation theory. The concept of this theory is the physical entanglement of a number of fillers to create a continuous path through the matrix. A too small load results in no connection between the fillers. By increasing the volume of fillers in the matrix, the probability of contact also rises. A path only exists if a sequence of fillers may be found from the begin to the end of the matrix. Several paths may be formed, but one path is already sufficient to have connection. This contact is mainly dependent on the positions of the fillers and the density of the matrix [32], [33].

Two different types of percolation can be distinguished, namely bond percolation and site percolation which are presented in Figure 15. In case of bond percolation, links are formed between the fillers while at site percolation, the fillers just touch each other without chemical bonding.
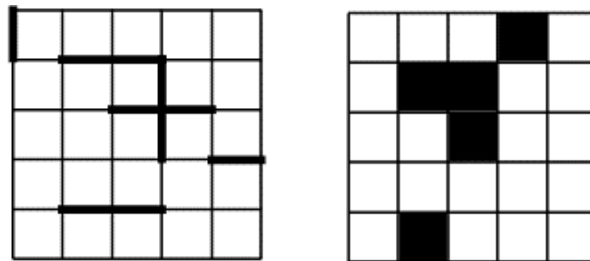
Figure 15: Different types of percolation: (left) bond percolation, (right) site percolation [34]

The connection of conductive fillers within a polymer matrix results in the production of continuous and conducting paths through it. Due to this, electrical conductivity can be generated in normally insulating polymers. Below a critical concentration, the conductive fillers are individually isolated in the matrix. By increasing the fraction of inclusions (fillers), connections are formed until a network construction appears through the matrix [35], [36].

For example, Figure 16 shows the conductivity as a function of the weight percentage of carbon black (conductive filler). In the vicinity of the insulator-conductor transition, the conductivity rises quickly, while it is relatively steady in the insulating and conductive zone. Thus, this S-shape curve obviously demonstrates the required filler amount to form conductive paths. Finally, the graph shows a very little decrease of conductivity at a very high concentration of carbon black. In this case, the particles obstruct each other in order that the existing conductive paths are interrupted [28].
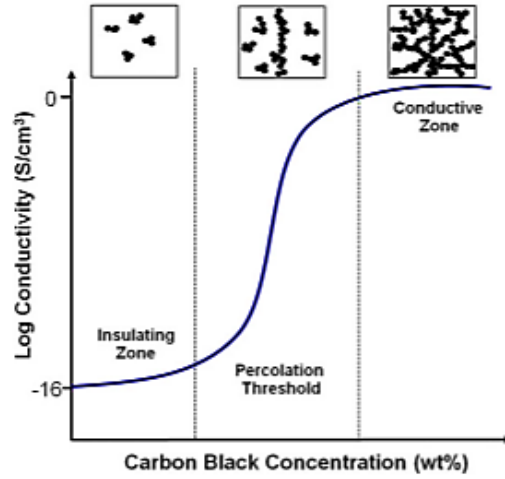
Figure 16: Schematic representation of logarithm of conductivity (S/cm³) versus carbon black concentration (wt%), illustrating a S-shaped percolation curve [28]

2.3 Percolation models

Scientists and mathematics attempt to model the percolation theory considering the random dispersion and the probability of connection between the fillers in the blend. A few percolation models are successfully created, which all characterize the connectivity properties in a disordered system. Electrical conductivity, diffusion and elasticity of composite materials are modelled, but the focus in this master's thesis is the transition of insulating to conducting polymer blends with increasing filler fraction. The experimentally results are compared with the modelled percolation threshold [37].

This paragraph firstly describes a general percolation model which approaches analytically and numerically the electrical percolation phenomenon, called the Power Law Model. After that, the Excluded Volume Model is explained, both for monodisperse and polydisperse rod networks. Finally, two specific percolations models are illustrated for spherical granulates, in particular carbon black.

2.3.1 Power Law Model

In the vicinity of the percolation threshold, the macroscopic electrical conductivity σ follows a power-law dependence:

$$\sigma \approx \sigma_0 * [\varphi - \varphi_c]^t \tag{2.1}$$

where φ is the filler concentration, φ_c is the critical percolation threshold and σ_0 is the intrinsic conductivity of the filler. The power law exponent t dependents on the filler connection and amounts ± 1,33 for 2D systems and ± 2 for 3D systems. However, the power law exponent varies with values as high as 10 and this nonuniversality is due to complex tunnelling transport processes in composites [28], [38].

The experimentally and theoretically studied power law model only approaches the electrical conductivity close to the percolation threshold. Furthermore, the model is just suitable for cylindrical particles like carbon nanotubes and metal nanowires (e.g. silver nanowires). This cylindrical shape, in particular the aspect ratio (L/D) and orientation of the fillers, influences the macroscopic electrical conductivity. Also the dispersion within the matrix affects the ultimate result [38], [39].

2.3.2 Excluded Volume Model

The most regularly used analytical percolation model is the excluded volume model (in combination with Monte Carlo simulations) where the percolation threshold of a blend is stipulated by the excluded volume (see Figure 17) of fillers. "The excluded volume of an object is defined as the volume around the object into which the center of mass of another identical object cannot enter without contacting the first object" [38, p. 17].
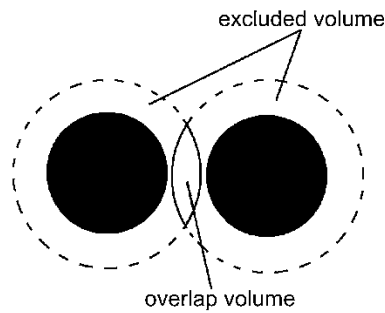
Figure 17: Illustration of excluded volume

The excluded volume model is expanded for fillers with an aspect ratio higher than 100. Furthermore, the model considers an arbitrary dispersal of fillers, but processing techniques can already align these fillers [38], [40]. Moreover, the model distinguishes between a monodisperse rod network and a polydisperse rod network, but both are based on the same expression. This equation demonstrates an inverse proportionality between the filler amount for analytical percolation and the excluded volume of a filler:

$$N_c \sim \frac{1}{V_{ex\_rod}} \qquad (2.2)$$

where V_{ex_rod} is the average excluded volume of a filler and N_c is the amount of fillers per unit volume required for percolation [38].

The average excluded volume of a filler is generally given by the following equation, where D and L are the diameter and length of the cylindrical filler respectively.

$$V_{ex\_rod} = \frac{\pi}{2}D\left[\frac{\pi}{4}D^2 + L^2\right] + \frac{\pi}{4}D^2L(3+\pi) \tag{2.3}$$

Monodisperse rod network

The particles in a monodispersed network all have an identical size without any deviation. To figure out the percolation threshold of these theoretical cylindrical particles, two different equations are discussed dependent on the aspect ratio (L/D) [38].

In case of a slender-rod limit (L/D → ∞), the percolation threshold is given by [38]:

$$\varphi_c = \frac{V_{rod}}{V_{ex\_rod}} = \frac{\frac{\pi}{4}D^2L}{\frac{\pi}{2}D\left[\frac{\pi}{4}D^2 + L^2\right] + \frac{\pi}{4}D^2L(3+\pi)} = \frac{1}{\frac{\pi}{2}\frac{D}{L} + 2\frac{L}{D}(3+\pi)} \tag{2.4}$$

where V_{rod} is the volume of a cylindrical particle.

When the monodispersed cylindrical particles have a finite aspect ratio (between 10 and 100), the percolation threshold is demonstrated as follows [38]:

$$\varphi_c = N_cV_{rod} = \frac{V_{rod}}{V_{ex\_rod}} = \frac{(1+s)\frac{\pi}{4}D^2L}{\frac{\pi}{2}D\left[\frac{\pi}{4}D^2 + L^2\right] + \frac{\pi}{4}D^2L(3+\pi)} \tag{2.5}$$

where s is an empirical correction factor. There are several estimations to this correction factor, but the principal equation is given by:

$$s = 3.2\left(\frac{R}{L}\right)^{0,46} \tag{2.6}$$

where R is the radius of the cylindrical particle.

Another expression for the correction factor is determined by Berhan and Sastry, namely [38]:

$$s = 5.23\left(\frac{L}{R}\right)^{-0,57} \tag{2.7}$$

Polydisperse rod network

The particles in a polydispersed network have different dimensions, ergo there is a (Gaussian) distribution in size. In this case, the equation of the percolation threshold is demonstrated as follows [38]:

$$\varphi_c = \frac{(1 + s_{poly}) \frac{\pi}{4} D_n{}^2 L_n}{\frac{\pi}{2} D_n \left[\frac{\pi}{4} D_n{}^2 + L_n{}^2\right] + \frac{\pi}{4} D_n{}^2 L_n (3 + \pi)} = \frac{(1 + s_{poly})}{\frac{\pi}{2} \frac{D_n}{L_n} + 2 \frac{L_n}{D_n}(3 + \pi)} \tag{2.8}$$

where D_n and L_n are the average diameter and length of the cylindrical particles respectively.

The empirical correction factor s_{poly} is also a function of the average length and diameter of the polydispersed particles, given by:

$$s_{poly} = 3,2 \left(\frac{D_n/2}{L_n}\right)^{0,46} \tag{2.9}$$

2.3.3 Other percolation models

A lot of percolation models are theoretically or experimentally determined, but they are mostly very complex mathematical models due to the (statistic) probability of the percolation theory. These models are too complicated for practical applications and for that reason, simplifications are performed. The following two percolation models are extremely simplified to get an understandable approximation for the percolation threshold of spherical granulates, in particular carbon black.

Percolation model for spherical granulates

Bruggeman *et al* proposed the efficient media theory, a mean field theory used to discuss spherical granulates compounding binary composites. In this theory, a random blend of spherical granular loads (all) the space of an insulated matrix. When the volume fraction and the intrinsic conductivity of the insulated matrix and spherical conductive fillers are known, the electrical conductivity can be calculated as follows:

$$\varphi_L \left(\frac{\sigma_L - \sigma_M}{\sigma_L + 2\sigma_M}\right) + \varphi_H \left(\frac{\sigma_H - \sigma_M}{\sigma_H + 2\sigma_M}\right) = 0 \tag{2.10}$$

In this expression is σ_M the electrical conductivity of the blend, φ_L and φ_H are the volume fraction of the insulated matrix and spherical granulates and σ_L and σ_H are the intrinsic conductivity of the insulated matrix and granulates respectively [41].

Percolation model for carbon black

A very simplified percolation model for (spherical) carbon black, developed by Janzen, describes an expression for the critical volume fraction of carbon black. This theoretically and

experimentally tested model is based on the average amount of connections between carbon black particles and is given by:

$$V_c = \frac{1}{1 + 4\rho v} \tag{2.11}$$

where V_c is the critical volume fraction, ρ is the density of carbon black and v is the dibutyl phthalate (DBP) absorption value in g/cm³. The dibutyl phthalate absorption value is the amount of DBP that carbon black can absorb before reaching a viscous paste [28], [42].

3 Materials

A conductive blend is prepared by mechanically blending two different materials, namely conductive fillers within a polymer matrix. Various material combinations are available, because both polymer matrix and conductive filler can differ. An optimal combination does not still exist and it is highly dependent on the required extensibility and conductivity of the blend.

3.1 Polymer matrix

The polymer matrix in this research includes elastomers, which are able to endure reversibly large elastic deformations due to their specific properties, namely a high yield strain and a low tensile modulus. Besides, the phase of an elastomer at room temperature is very favourable because the temperature is above the glass transition temperature (T_g). Due to this, the elastomeric matrix has viscoelastic properties and ergo a very high ductility. Moreover, elastomers consist of a network of long chain molecules which are entangled by crosslinks. This structure either results in the reversible way of stretching and recovering the initial shape of the elastomer [43].

Frequently used elastomers in polymer blends are polyurethanes, silicones and acrylics. This research deals with the most widely used silicone, namely polydimethylsiloxane. In addition, the use of a self-healing elastomeric matrix is explained.

3.1.1 Polydimethylsiloxane (PDMS)

Polydimethylsiloxane is a silicone elastomer consisting of a polymer backbone of alternating silicon and oxygen atoms, as shown in Figure 18. It is synthesized from water and dimethyldichlorosilane by a polymerisation reaction.
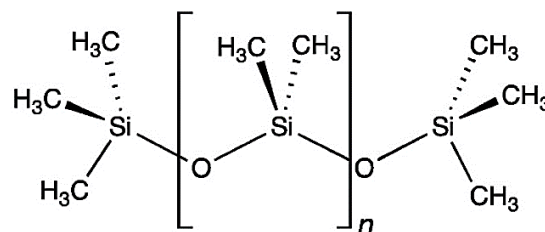
Figure 18: Structural formula of polydimethylsiloxane

PDMS is a transparent and viscoelastic silicone, which is also chemically inert and thermally stable. Moreover, it has good dielectric properties, a good ozone resistance and a huge flame resistance. These outstanding properties are due to the high strength of the silicon-oxygen bond, namely 451 kJ/mole. Finally, polydimethylsiloxane is easily shaped because of the flowability at room temperature [44], [45], [46].

3.1.2 Self-healing polymers

The possible occurrence of little cracks arising in the conductor while stretching results in a debilitation of the conductor until overall fracture and loss of conductivity occurs. These little cracks and damage can be repaired without external aid by using a self-healing elastomeric matrix. Due to the ability to self-heal mechanical damage, the lifetime, the reliability and the durability of the polymer matrix increase [47].

Recently, a few self-healing polymers are developed that have exciting applications toward electronic skins, functional surfaces and electrical conductors. In this master's thesis, the emphasis is put on the evolvement of a self-healing elastomeric matrix to create a conductive self-healing blend.

Guo *et al.* described a conductive composite by combining poly(2-hydroxyethyl methacrylate) (PHEMA) and single-walled carbon nanotubes (SWCNT's) through host-guest interactions. The PHEMA-SWCNT composite is able to self-heal without external aid under ambient conditions and combines electrical conductivity and extensibility [48]. Another self-healing conductive hydrogel is fabricated by the in situ doping of poly(N-acryloyl glycinamide-co-2-acrylamide-2-methylpropanesulfonic) (PNAGA-PAMPS) hydrogels with poly(3,4-ethylenedioxythiophene) polystyrene sulfonate (PEDOT/PSS). The reconstruction of hydrogen bonds during cyclic heating and cooling leads to the self-healability of the hydrogel [49]. Montarnal *et al.* described a last option to synthesise a self-healing elastomer from vegetable oil, fatty-acid derivatives, diethylene triamine and urea. "A wide molecular distribution of randomly branched oligomers equipped with self-complementary hydrogen bonding groups" results in the preparation of supramolecular networks with associating moieties [3, p. 7925].

3.2 Conductive fillers

Each distinctive conductive filler influences the properties of a blend, especially the electrical conductivity and the viscosity. Ergo, it is important to discuss each filler separately, more specifically the influence of the quantity of conductive fillers on the blend properties. The most essential characteristic in this master's thesis is the percolation threshold of each conductive filler, which should be passed to create a conductive elastomeric matrix. Further, the processability of a conductive blend (ink) depends on the viscosity. A too high viscosity inhibits the blend deposition to produce stretchable conductors.

Six different conductive fillers are discussed in this master's thesis, namely carbon black (CB), multi-walled carbon nanotubes (MWCNT's), silver nanowires (Ag NW's), silver microparticles (Ag MP's), silver coated copper flakes (Ag-Cu flakes) and a mixture of carbon black nanopowder and carbon nanotubes. Other possible conductive fillers are graphene, nickel powders, gold particles, copper microparticles, single-walled carbon nanotubes,… but these are not discussed in this thesis.

3.2.1 Carbon black (CB)

Carbon black, which are finely divided particles of amorphous carbon, can be produced by an incomplete combustion or a thermal decomposition of gaseous or liquid hydrocarbons like coal-tar pitch, oil or natural gas under controlled conditions. The obtained spherical particles, whose characteristics depend on the manufacturing process, are finally dried and ready for use, mainly as filler material in car tires. In addition, carbon black is implemented as black pigments in paint, printing ink and carbon paper, but it is also used in plastics and protective coatings [50], [51].

The use of carbon black as conductive fillers within a polymer matrix has already been studied and literature offers some guide values of the percolation threshold of carbon black. Table 1 shows several percolation thresholds (volume percentage of carbon black) in a polymer matrix, but this value highly depends on different properties (such as intrinsic electrical conductivity and particle size) of the carbon black powders and the polymer matrix [52], [53].

Table 1: Percolation thresholds of carbon black in a polymer matrix.

Volume percentage CB (vol%)	Polymer matrix
7.8	Polypropylene (PP)
10	High density polyethylene (HDPE)
8	Natural Rubber (NR)

Table 1 demonstrates that the percolation threshold of carbon black is around 8-10 vol%, but this value can deviate. Each carbon black powder has to be tested individually to determine the percolation threshold, because the powders have different properties.

3.2.2 Multi-walled carbon nanotubes (MWCNT's)

Multi-walled carbon nanotubes are composed of multiple concentric cylinders of graphene, as shown in Figure 19. Each concentric tube, called a single-walled carbon nanotube, is an allotrope of sp^2 hybridised carbon (six-membered nucleus).
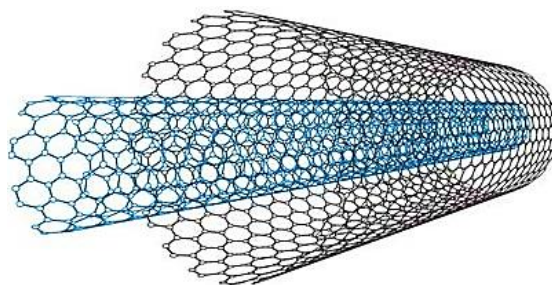
Figure 19: Illustration of multi-walled (double) carbon nanotubes [54]

In general, multi-walled carbon nanotubes have outstanding properties such as a high chemical and thermal stability. In addition, MWCNT's have a large tensile strength and can rise the strength of a composite significantly. Finally, they have a high aspect ratio and low electrical resistance in order that MWCNT's are (theoretically) superb conductive fillers [55].

Due to the excellent conditions of MWCNT's as conductive filler, a lot of research is already performed to determine its percolation threshold in different polymer matrices (shown in Table 2) [56], [57], [58], [59].

Table 2: Percolation threshold of multi-walled carbon nanotubes in a polymer matrix

Weight percentage MWCNT's (wt%)	Polymer matrix
0.675	Polyvinyl alcohol (PVA)
0.6	Polydimethylsiloxane (PDMS)
0.35	Polycarbonate polybutylene terephthalate
1.5	Polydimethylsiloxane (PDMS)

The percolation thresholds of multi-walled carbon nanotubes are similar in order of magnitude, but there is still a little difference between them due to the size (especially aspect ratio) of the cylindrical nanotubes. Longer nanotubes have a higher conductivity (and lower percolation threshold), because connections between the fillers are formed simpler [60].

3.2.3 Silver nanowires (Ag NW's)

Silver nanowires are synthesized via different methods, such as "a reduction of $AgNO_3$ in ethylene glycol solutions containing poly(vinylpyrrolidone) (PVP), a synthesis in aqueous solutions in the presence or absence of seeds and surfactants, a hydrothermal synthesis using glucose as reducing agent and a microwave-assisted synthesis" [16, p. 2423].

Silver is the best conductive metal (better than copper or gold) in order that a very high electrical conductivity is obtained by the use of silver nanowires. Furthermore, the shape of the nanowires results in the simple formation of conductive paths through a polymer matrix. The connections between filamentous structures (e.g. silver nanowires) are created easier and faster than between spherical granules (e.g. silver microparticles), as shown in Figure 20. Due to this, less silver nanowires are needed to generate a certain electrical conductivity [61].
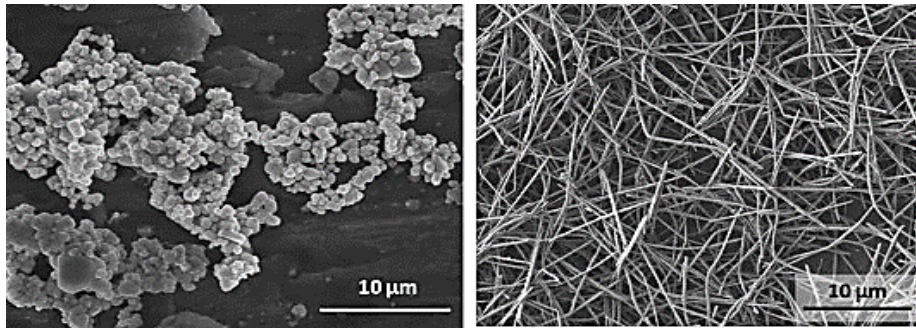
Figure 20: (left) SEM image of silver microparticles, (right) SEM image of silver nanowires [62]

Though silver nanowires are excellent conductive fillers, the use is rather limited due to the high cost-price. Some studies are already performed to find out the percolation threshold (Table 3), but this value depends on the size of the nanowires, the manufacturing method and the polymer matrix [16], [61], [62].

Table 3: Percolation threshold of silver nanowires in a polymer matrix

Volume percentage Ag NW's (vol%)	Polymer matrix
0.5 - 0.75	Polystyrene (PS)
2.2	Poly(vinylidenefluoride-co-trifluoro-ethylene) P(VDF-TrFE)
0.6	Poly(vinylidenefluoride-co-trifluoro-ethylene) P(VDF-TrFE)
1.8	Polyvinylidene fluoride (PVDF)

3.2.4 Silver microparticles (Ag MP's)

Silver microparticles have a very good electrical conductivity and are suitable for paint additives and as conductive filler material. In the last option, the percolation threshold is highly dependent on the used polymer matrix and the size of the silver particles [63].

Table 4 shows the results of two percolation experiments which give two guide values for the percolation threshold of silver microparticles [62], [64].

Table 4: Percolation thresholds of silver microparticles in a polymer matrix

Volume percentage Ag MP's (vol%)	Polymer matrix
13	P(VDF-TrFE)
6	Epoxy composites

3.2.5 Silver coated copper flakes (Ag-Cu flakes)

Ag-Cu flakes consist of a copper nucleus coated with a silver layer and form an alternative filler material for pure silver particles. The high electrical conductivity, the good quality and the cost-price are the biggest advantages to employ these flakes as conductive filler [65]. Chuang *et al.* established the percolation threshold of the Ag-Cu flakes in a PDMS matrix, as shown in Table 5 [66].

Table 5: Percolation threshold of silver coated copper flakes in a polymer matrix

Volume percentage Ag-Cu flakes (vol%)	Polymer matrix
26.28	Polydimethylsiloxane (PDMS)

3.2.6 Mixture of carbon black nanopowder and carbon nanotubes

This conductive filler consists of a mixture of carbon nanotubes and carbon black nanopowder. Carbon black can generate a high electrical conductivity in a polymer blend, while CNT's have magnificent physical properties, especially a high aspect ratio and also a low intrinsic resistance. The combination of both fillers in a polymer matrix can result in a low percolation threshold [67].

The mixture of carbon black nanopowder and carbon nanotubes has been tested a few times as conductive filler material and thus, its percolation threshold in some polymer matrices is already determined, as shown in Table 6 [67], [68].

Table 6: Percolation thresholds of mixture CB & CNT's in a polymer matrix

Weight percentage CB + CNT's (wt%)	Polymer matrix
1	Epoxy composites
1 – 3	Unknown (not reported)

The percolation threshold in Table 6 shows a good guide value, but it depends highly on the intrinsic electrical conductivity of the fillers, the polymer matrix and the load distribution between carbon black and carbon nanotubes [69].

4 Percolation experiment

4.1 Introduction

The objective of the percolation experiment is to measure the percolation threshold of six different conductive fillers, namely carbon black (CB), multi-walled carbon nanotubes (MWCNT's), silver nanowires (Ag NW's), silver microparticles (Ag MP's), silver coated copper flakes (Ag-Cu flakes) and a mixture of carbon black nanopowder and carbon nanotubes. These conductive fillers are separately blended with polydimethylsiloxane (PDMS), a high viscous elastomer.

The amount of the conductive fillers in the PDMS matrix is increased gradually while the resistance of the blend is measured in situ with a four-wire measurement. Besides, it is important that the particles are mixed well with the elastomeric matrix by decreasing the viscosity of the blend. A hot oil-bath is used to reduce the blend viscosity, because a higher temperature leads to a lower viscosity.

The resistance of the blend decreases quickly at a certain volume percentage of conductive fillers and thus, the percolation threshold is accomplished.

4.2 In situ measurement of blend resistance

Nowadays, literature does not describe any in situ measurement to determine the resistance of a blend. Generally, a sample of the blend is taken, poured into a mould and cured. After curing, the electrical resistance is measured one time by a two- or four-wire measurement.

In this master's thesis, an in situ measuring tool is designed to determine the blend resistance during the whole experiment. This continuous measurement involves two interesting advantages instead of a single measurement.. On the one hand, the blend resistance is measured each second resulting in a lot of measuring points per addition. On the other hand, it is possible to observe the required mixing time per addition of conductive fillers. When the blend resistance is a constant value, the conductive fillers are mixed well in the blend and the fillers load can be increased.

The design of the measuring electrode is based on a four-wire resistance measurement in order that the cable- and contact resistances are minimized. Due to this design, the influence on the total resistance is reduced and low resistances are measured accurately, which is absolutely necessary in this investigation [70].

At the beginning of the investigation, the measuring electrode was created manually though the measuring results were not meticulous. The second idea was the attachment of tungsten electrodes in the bottom of a round bottom flask that resulted in correct measurements. Both measuring tools are described in the following paragraphs.

4.2.1 Handmade measuring electrode

The design of the handmade measuring electrode (Figure 21) was based on a four-wire measurement to reduce the cable- and contact resistances. It was constructed of copper tape with a thickness of 60 µm.

Figure 21: Design of handmade measuring electrode

A strip of the copper tape was stuck on clay coated kraft paper with a silicone layer (Grafityp, product type: CCK C-liner 30-35), consisting of 35% controlled release agent (CRA). Next, the electrode was cut out by using the 'Roland Camm-1 Servo' vinyl cutter. The cutting force was set to 100 gf (gram force) while the cutting speed did not affect the electrode design. Afterwards, the excess of copper tape was removed to obtain the measuring electrode (Figure 22).
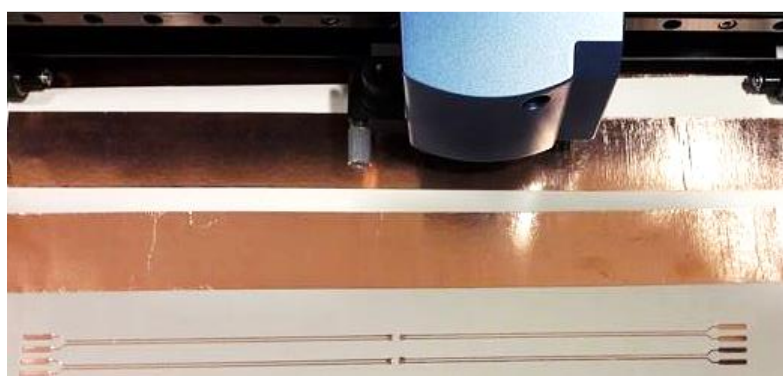
Figure 22: Production of copper electrodes by a vinyl cutter

In the next stage of the construction, the contact points of the excised electrode were coated with 'WD-40 multispray' and the electrode was surrounded completely by carbon tape. Due to the coating layer, it was simpler to uncover the contact points with a scalpel. Unfortunately, this production step was very time-consuming and it also damaged the contact points. Subsequently, the flexible measuring electrode was covered with PDMS, attached into a round bottom flask and cured at 140°C (Figure 23).

Figure 23: Handmade measuring electrode in round bottom flask

In the last step, the contact points were connected to a Keithley 2000 multimeter and the measurements were collected in LabVIEW. Though the blend resistance was measured in situ, the results were not accurate because of the damaged contact points.

4.2.2 Round bottom flask with built-in tungsten electrodes

To obtain reproducible and accurate measurements, it was essential to design an identical measuring electrode for each percolation experiment. For this purpose, four tungsten pins (electrodes) were attached through the bottom of a 50 ml round bottom flask. The distance between the contact points in the flask is 2 mm.

A crucial parameter of this design is the difference between the thermal expansion coefficient of the electrodes and the flask. It is important that both materials have an equivalent coefficient of expansion to avoid stresses in the measuring flask. Due to this, tungsten electrodes were selected, because its thermal expansion coefficient is $4.5*10^{-6}$ K^{-1} and estimates highly the value of borosilicate glass ($3.3*10^{-6}$ K^{-1}). Other metal pins (such as copper or aluminium) were not suitable because of the too high coefficient of thermal expansion. Besides, the measuring flask (Figure 24) was cooled down gradually to reduce the residual stresses of the construction.

Figure 24: Round bottom flask with built-in tungsten electrodes: (left) front view, (right) top view

This round bottom flask with built-in tungsten electrodes measured accurately the resistance of the blend, because the electrodes were not damaged and the four-wire measurement minimised the cable- and contact resistances.

4.2.3 Complete measuring setup

The complete measuring equipment (Figure 25) consists of the round bottom flask with built-in tungsten electrodes which is connected to a Keithley 2000 multimeter with an upper measurement limit of 120 MΩ (non-conductive blend). This setup measures in situ (each second) the blend resistance and saves the results in LabVIEW.

Furthermore, a hot oil bath heated up the blend to 85 ± 1°C to decrease the viscosity, because a higher temperature leads to a lower viscosity. Due to this reduction, the conductive fillers were mixed simpler in the elastomeric matrix by the use of a non-conductive stirrer. It was essential to cover the stirrer stick with a conformal isolating coating layer (Kontakt Chemie – Plastik 70) in order that it had no influence on the measurements.
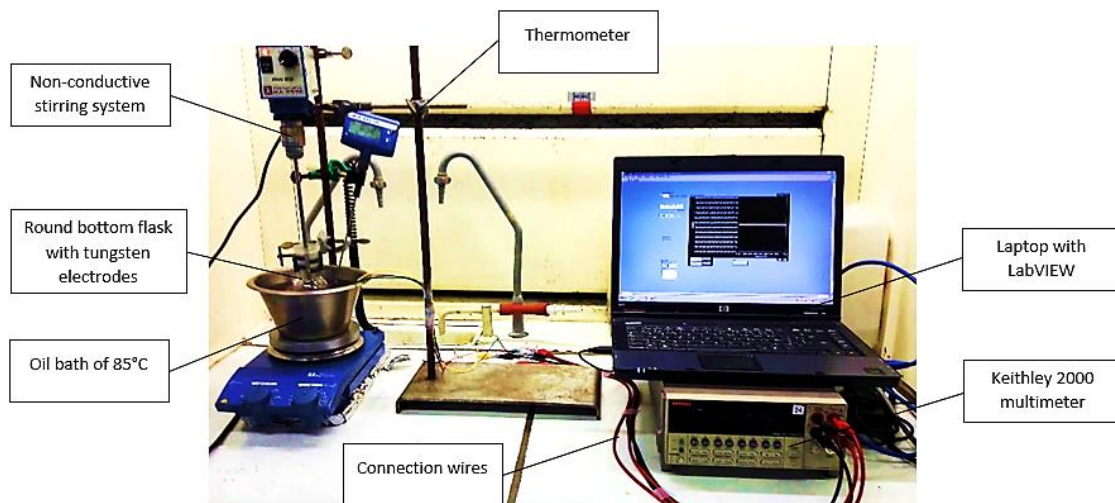
Figure 25: Complete measuring setup of the percolation experiment

4.3 Percolation threshold of conductive fillers

Following paragraph describes the observed percolation threshold of the different conductive fillers in a PDMS-matrix (Dow Corning – Sylgard 184). The required volume percentage to pass the percolation threshold and the corresponding resistance are quantified.

4.3.1 Carbon black in PDMS-matrix

Micron super adsorption activated porous carbon powder (US Research Nanomaterials, product no: US 1143M) is used as conductive filler material. These particles are produced from coconut shells at a carbonisation temperature above 1300°C and obtain the following properties (as shown in Table 7) [71].

Table 7: Characteristics of carbon black powder

Characteristics CB	Value
Average diameter	10 µm
Density	0.47 g/ml
Intrinsic electrical resistivity	0.32 Ω.cm

Initially, the required mixing time of the particles in a PDMS-matrix was determined by measuring the blend resistance as a function of the mixing time (Figure 26). An excess of particles was directly added into a PDMS-matrix while the blend was mixed to obtain a steady blend resistance. The amount of particles was calculated from the preparation of the percolation experiments and it amounted ± 40 vol% carbon black (in PDMS).
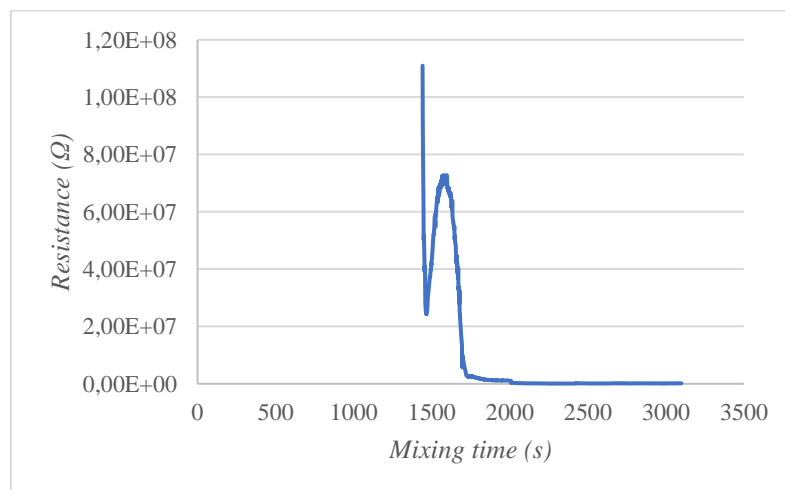
Figure 26: Determination of optimal mixing time of particles in PDMS-matrix

Figure 26 shows that the resistance of the blend remains constant after ± 2450 s (41 min). Due to this experiment, an overestimation of the average mixing time was made and set to 45 min to ensure that a homogenous blend was formed. Thus the volume percentage of the carbon

black particles in a PDMS-matrix was risen every 45 min while the blend resistance was measured in situ, as shown in Table 8.

Table 8: Resistance and logarithm of resistance per volume percentage carbon black

Volume percentage CB (vol%)	Resistance (Ω)	Logarithm of resistance (Ω)
0	No value[1]	No value
20.79	No value	No value
37.12	No value	No value
44.05	No value	No value
50.30	No value	No value
53.21	No value	No value
55.98	No value	No value
58.63	79017102	7.90
61.16	823097	5.92

The resistance of the blend slightly decreases at 58.63 vol% carbon black, but the percolation threshold is still not passed. When the amount of carbon black is increased to 61.16 vol%, the resistance lowers 100x in order of magnitude. Unfortunately, the percolation experiment had to be finished at this amount of carbon black, because the viscosity of the blend did not tolerate any extra addition: the blend was too viscous which caused a lot of friction on the measuring electrodes. The blend temperature was risen to 100°C to reduce the viscosity with no effect. For that reason, the percolation experiment was finished in order that the measuring flask would not be destructed.

The small observed decrease in electrical resistance is demonstrated in Figure 27 by the expression of the logarithm of the resistance as a function of the volume percentage carbon black. Although the most measurements points resulted in 'no value', this measurement result was set to the upper limit of the Keithley 2000 multimeter (120 MΩ). Due to this incorrect valuation, Figure 27 demonstrated obviously the drop in electrical resistance.

---

[1] 'No value' means that the blend resistance was higher than the upper measurement limit (120 MΩ) of the Keithley 2000 multimeter.
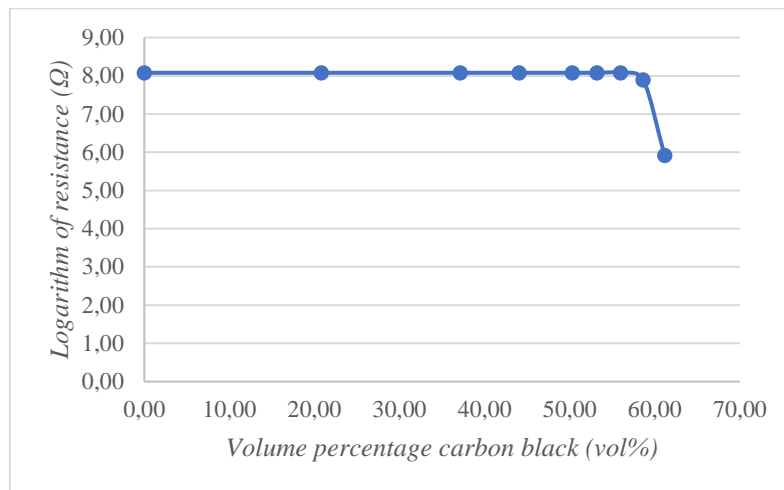
Figure 27: Logarithm of resistance as a function of volume percentage CB

Figure 27 shows that the percolation threshold of carbon black in PDMS was estimated, but it was not passed at 61.16 vol% of carbon black. Due to this, the final resistance of the conductive blend could not be determined. Although the exact percolation threshold was not reached, it is at least 6x larger in order of magnitude than the described values in literature (8 - 10 vol%). Possible causes for this are a difference between the intrinsic conductivity, the size of the particles and the viscosity of the blend.

4.3.2 Multi-walled carbon nanotubes in PDMS-matrix

Multi-walled carbon nanotubes (Sigma-Aldrich, product no: 659258) are examined in this master's thesis and the main characteristics of this conductive filler material are shown in Table 9 [72].

Table 9: Characteristics of multi-walled carbon nanotubes

Characteristics MWCNT's	Value
Diameter	110 - 170 nm
Length	5 - 9 µm
Density	1.7 g/ml

The volume percentage of the multi-walled carbon nanotubes was increased every 45 minutes in a PDMS-matrix while the blend resistance was measured in situ. Table 10 shows the measured resistance per volume percentage multi-walled carbon nanotubes.

Table 10: Resistance and logarithm of resistance per volume percentage multi-walled carbon nanotubes

Volume percentage MWCNT's (vol%)	Resistance (Ω)	Logarithm of resistance (Ω)
0	No value	No value
0.66	No value	No value
1.31	No value	No value

1.98	No value	No value
2.65	No value	No value
3.32	No value	No value
4.68	92065167	7.96
5.40	59640	4.78
6.11	1763	3.25

The logarithm of the resistance as a function of the volume percentage multi-walled carbon nanotubes is represented graphically in Figure 28. It demonstrates distinctly the drop in electrical resistance at the percolation threshold.
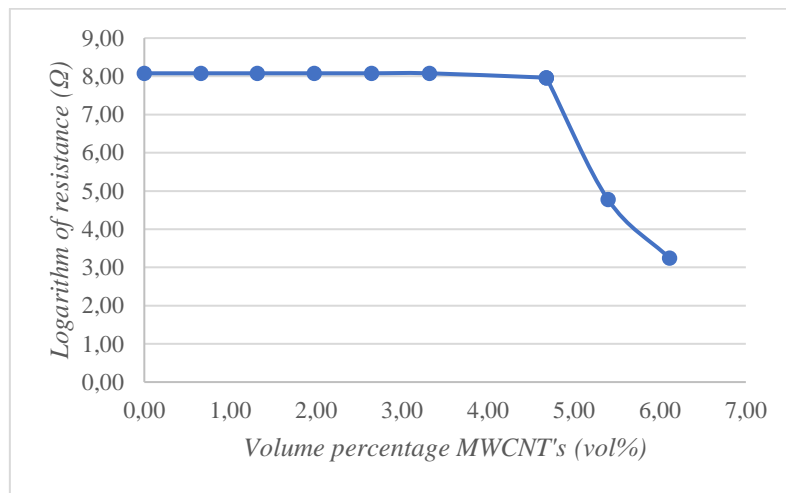
Figure 28: Logarithm of resistance as a function of volume percentage MWCNT's

Figure 28 shows that the percolation threshold of MWCNT's in a PDMS-matrix is around 5.40 vol%. This value is 10x smaller than the percolation threshold of carbon black due to the shape of the particles. The cylindrical MWCNT's have a bigger probability to form conductive paths through the matrix than the spherical carbon black. For that reason, a smaller volume percentage of MWCNT's is sufficient to pass the percolation threshold. The final resistance at 6.11 vol% - namely 1763 Ω - is still too high for the application in electronic conductors (1 Ω).

4.3.3 Silver nanowires in PDMS-matrix

In this experiment, silver nanowires (RAS AG, product no: ECOS HC) are tested as conductive filler material which characteristics are represented in Table 11 [73].

Table 11: Characteristics of silver nanowires

Characteristics Ag NW's	Value
Diameter	30 - 50 nm
Length	10 - 40 µm
Density	10.49 g/ml

The silver nanowires were dispersed in ethylene glycol (3 wt% Ag NW's) to prevent agglomeration, but the solvent influenced the final measurement result. Due to this, ethylene glycol had to be evaporated during the experiment to obtain the percolation threshold accurately. Unfortunately, the boiling point of ethylene glycol is ± 197°C in order that the blend temperature should be increased from 85°C until 200°C. This rise in temperature required an alternative measuring flask with Teflon wires, as shown in Figure 29. These wires could resist a temperature of 200°C without any degradation.

Figure 29: Round bottom flask with built-in electrodes and Teflon wires

The silver nanowires load was increased every 2 hours (instead of 45 minutes), because the ethylene glycol had to be evaporated. Meanwhile, the resistance of the blend was measured in situ, but the blend remained insulating during the experiment. Due to a shortage of silver nanowires, the percolation threshold was not reached and the final volume percentage of silver nanowires in PDMS amounted 2.07 vol%. This experiment shows that the percolation threshold of the tested silver nanowires is higher than 2.07 vol%, but the exact value is still unknown.

4.3.4 Silver microparticles in PDMS-matrix

Silver microparticles (Metallpulver, product no: 24000) are used to determine their percolation threshold. The main characteristics of these conductive fillers are represented in Table 12 [63].

Table 12: Characteristics of silver microparticles

Characteristics Ag MP's	Value
Average diameter	63 µm
Density	10.49 g/ml
Silver content	99.9 wt%

The silver microparticles load in a PDMS-matrix was extended every 45 minutes and meanwhile, the resistance of the blend was measured in situ. Unfortunately, the percolation threshold was not reached during this experiment, because of a shortage of silver microparticles. Though the volume percentage of silver microparticles amounted 37.50 vol%, the blend was still insulating. Due to the large particle size (diameter = 63 µm), it is more difficult to create a continuous and conducting path of the silver microparticles through the PDMS-matrix instead of smaller particles [17].

4.3.5 Silver coated copper flakes in PDMS-matrix

The characteristics of the used silver coated copper flakes (Metallpulver24, product no: 18046) in this master's thesis are shown in Table 13 [65].

Table 13: Characteristics of silver coated copper flakes

Characteristics Ag-Cu flakes	Value
Average diameter	D90 - 9 µm (90% < 9 µm)
Density	9.34 g/ml
Copper content	75 wt%
Silver content	25 wt%

Every 45 minutes, the volume percentage of the silver coated copper flakes was increased in a PDMS-matrix while the blend resistance was measured in situ, as shown in Table 14.

Table 14: Resistance and logarithm of resistance per volume percentage silver coated copper flakes

Volume percentage Ag-Cu flakes (vol%)	Resistance (Ω)	Logarithm of resistance (Ω)
0	No value	No value
2.90	No value	No value
7.37	No value	No value
10.66	No value	No value
15.18	No value	No value
18.14	26.5	1.42

The resistance of the blend reduces strongly at 18.14 vol% of Ag-Cu flakes and thus, the percolation threshold is passed. This phenomenon is distinctly shown in Figure 30 by the expression of the logarithm of resistance as a function of the volume percentage.
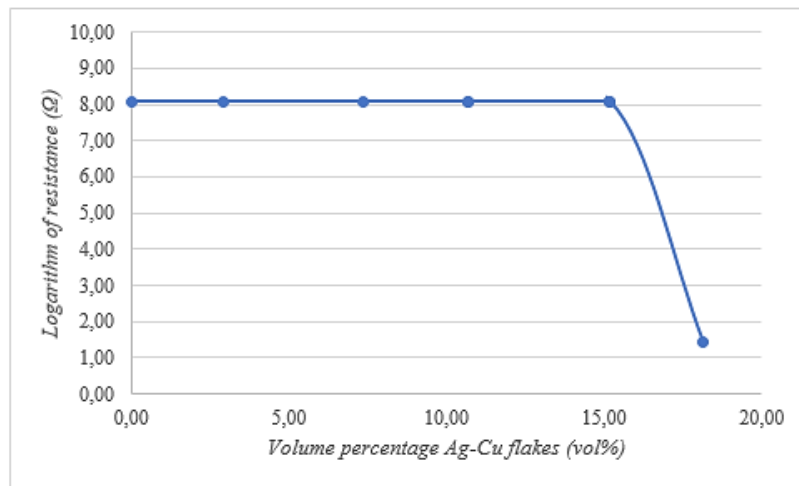
Figure 30: Logarithm of resistance as a function of volume percentage Ag-Cu flakes

The percolation threshold of Ag-Cu flakes in PDMS is between 15.18 and 18.14 vol% filler load with a final average resistance of 26.5 Ω. Though the percolation threshold was established clearly, it was very difficult to create a homogenous blend. Initially the Ag-Cu flakes did not mix in the matrix at 18.14 vol%. To reduce the blend viscosity, the temperature was risen to 110°C and 10 ml tetrahydrofuran (THF) was added. After the evaporation of THF, the Ag-Cu flakes were mixed well in the PDMS-matrix. Unfortunately, the experiment had to be finished at this volume percentage of Ag-Cu flakes, because the blend viscosity obstructed the creation of a homogenous blend and caused a lot of friction on the electrodes.

4.3.6 Mixture carbon black nanopowder and carbon nanotubes in PDMS-matrix

A mixture (with unknown mixing ratio) of super conductive carbon black nanopowder and carbon nanotubes (US Research Nanomaterials, product no: US4899) is tested. Table 15 shows the characteristics of this conductive filler material [68].

Table 15: Characteristics of mixture carbon black and CNT's

Characteristics CB + CNT's	Value
Diameter CB	5 - 100 nm
Diameter CNT's	30 - 100 nm
Length CNT's	5 - 30 µm
Density	0.15 g/ml
Intrinsic electrical resistivity	2 - 5 x 10^{-4} Ω.cm

Increasing the volume percentage of the carbon black and CNT mixture in a PDMS-matrix results in following measurement values, as shown in Table 16.

Table 16: Resistance and logarithm of resistance per volume percentage carbon black & CNT's

Volume percentage CB & CNT's	Resistance (Ω)	Logarithm of resistance (Ω)
0	No value	No value
13.19	No value	No value
23.65	No value	No value
25.86	No value	No value
28.04	13076	4.12
30.13	276	2.44
35.91	73	1.86

The blend resistance decreases strongly at 28.04 vol% of conductive fillers and thus, the percolation threshold is reached. This drop in electrical resistance is graphically demonstrated in Figure 31.
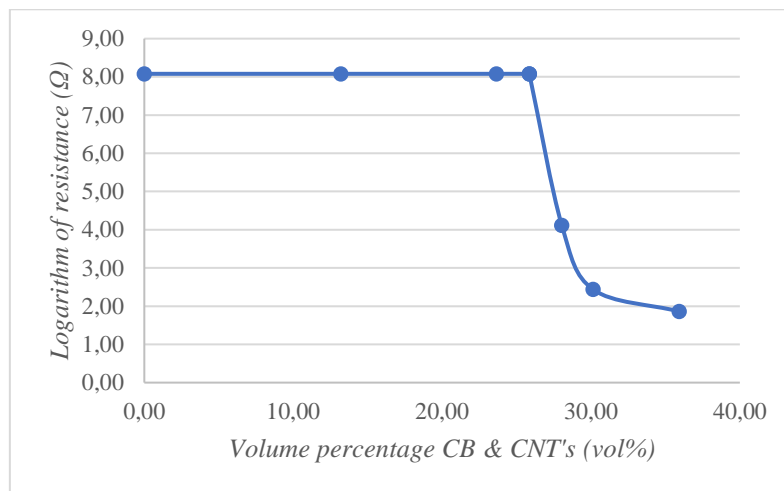
Figure 31: Logarithm of resistance as a function of volume percentage of carbon black and CNT's

After passing the percolation threshold, the blend resistance still decreases slightly by increasing the volume percentage of the CB & CNT mixture. At 35.91 vol%, the resistance is approximately constant and thus, the minimal value is reached. Due to this, an expand of filler load will not reduce the blend resistance anymore but it will only rise the viscosity and cost-price of the blend.

4.4 Comparison of conductive fillers

This paragraph compares the percolation threshold of the different conductive particles and the corresponding resistance in order to select the best conductive filler by minimizing the blend resistance and the cost-price.

4.4.1 Resistance of conductive fillers

The finally obtained volume percentage of each conductive filler in a PDMS-matrix and its corresponding blend resistance are represented in Table 17.

Table 17: Finally obtained resistance of each percolation experiment

Conductive filler	Volume percentage (vol%)	Resistance (Ω)
CB	61.16	823097
MWCNT's	6.11	1763
Ag NW's	2.07	No value
Ag MP's	37.50	No value
Ag-Cu flakes	18.14	26.5
CB & CNT's	35.91	73

Table 17 clearly shows that the percolation threshold of the silver nanowires and the silver microparticles was not reached during the experiments. Due to this, both conductive fillers are no longer discussed in this paragraph. In addition, the obtained blend resistance of the PDMS-matrix with carbon black and the PDMS-matrix with multi-walled carbon nanotubes is far too high to create a conductive blend. A low intrinsic electrical conductivity of the particles and a too small filler load are possible causes of this. The lowest blend resistances were achieved by the addition of silver coated copper flakes or the mixture of carbon black and carbon nanotubes. Unfortunately, the resistance of both is still too high for electronic applications (max. 1 Ω). An extra addition of conductive fillers could reduce the blend resistance, but the viscosity did not tolerate it (as previously discussed).

Furthermore, the percolation experiments passed (or estimated) the percolation threshold of 4 conductive fillers, namely carbon black, MWCNT's, Ag-Cu flakes and the mixture of carbon black and CNT's. Figure 32 demonstrates graphically the drops in electrical resistance by the expression of the logarithm of resistance as a function of the volume percentage conductive fillers.
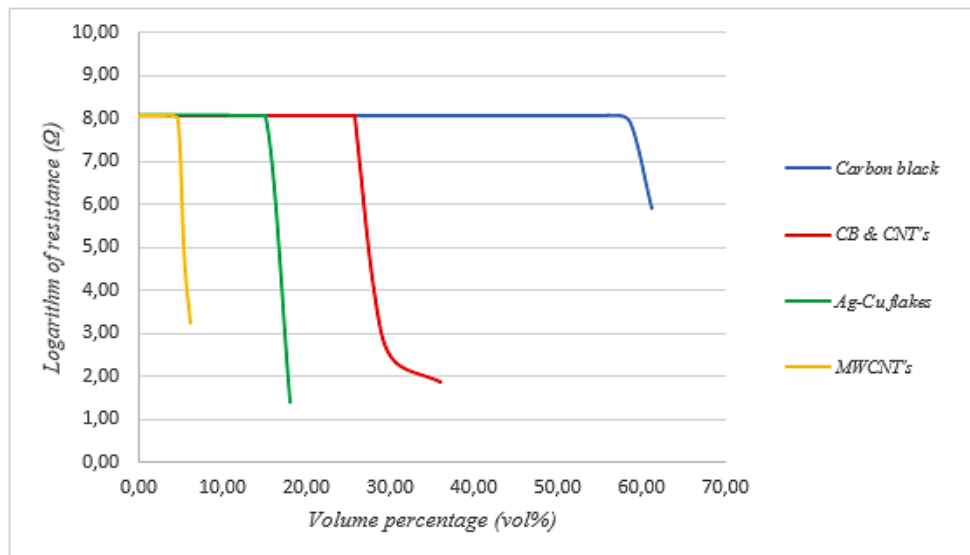
Figure 32: Comparison of percolation threshold of conductive fillers

This graph shows that the percolation threshold increases in the order of multi-walled carbon nanotubes, silver coated copper flakes, mixture of carbon black and carbon nanotubes and carbon black. The percolation threshold of MWCNT's is the lowest, because the cylindrical MWCNT's have a bigger probability to form conductive paths through the matrix than the other spherical particles. In addition, it is not only the shape and size of the particles that influence the percolation threshold. The Ag-Cu flakes and the carbon black particles approximately have the same diameter, namely 9 µm and 10 µm respectively. Yet there is a big difference between both percolation thresholds due to the intrinsic conductivity of the particles. Metal particles (e.g. Ag-Cu flakes) have a lower intrinsic resistance than carbon-based particles, resulting in a better conductivity (and smaller percolation threshold).

4.4.2 Optimal conductive filler

The optimal conductive filler and its concentration in the blend are selected by a trade-off between the desired resistance (max. 1 Ω) and the cost-price. Although 6 conductive fillers were tested, none met the requirements of the desired resistance. Due to this, the 2 best conductive fillers (resulting in the lowest blend resistance) are compared, namely the silver coated copper flakes and the mixture of carbon black and carbon nanotubes.

The comparison of the finally obtained (average) blend resistances shows that the silver coated copper flakes in PDMS (26.5 Ω) are more conductive than the mixture of carbon black and carbon nanotubes in PDMS (73 Ω). In addition, the PDMS-matrix with silver coated copper flakes is 35% more expensive than the PDMS-matrix with carbon black and carbon nanotubes. Taking into account the blend resistance and more restricted the cost-price of the fillers, it was decided to prefer the silver coated copper flakes as 'optimal' conductive filler. The triggering factor of this selection is the blend resistance, which has to be as low as possible for electronic applications.

54

5 Conductive self-healing polymer (CoSPo)

5.1 Synthesis of self-healing polymer

A self-healing elastomer has the possibility to heal little cracks spontaneously without external aid. Recently, a self-healing elastomer was created via a two-step synthesis starting from Pripol 1017 (cas no: 60-33-3), dipropylene triamine (DPTA) (cas no: 56-18-8) and solid urea (cas no: 57-13-6). Multiple functional groups are formed during this synthesis, which are capable of associating via parallel hydrogen bonds [3].

The self-healability of the synthesized polymeric network is caused by the large number of weak hydrogen bonds. While stretching the elastomeric network, some mechanical damage (cracks) can occur resulting in breaks of the weak hydrogen bonds instead of the (stronger) covalent bonds. These cracks are healed by the dynamic association and dissociation of the broken hydrogen bonds. Moreover, the polymer chains can be reconstructed on the damaged interfaces, because of the low glass transition temperature (T_g) of the polymer, which is below room temperature. Due to these 2 reasons, the synthesized polymer is capable to self-heal under ambient temperatures [3], [74].

5.1.1 Condensation polymerisation of dipropylene triamine (DPTA) with acid mixture

In the first synthesis step, 51.97 g Pripol 1017 (Croda Lubricants) was condensed with 25.97 g dipropylene triamine (Janssen Chimica NV) to create randomly branched oligomers. Pripol 1017 is a mixture of vegetable oil fatty acid derivatives with a composition of 2% mono-acid, 79% di-acid and 19% tri-acid, as shown in Figure 33.
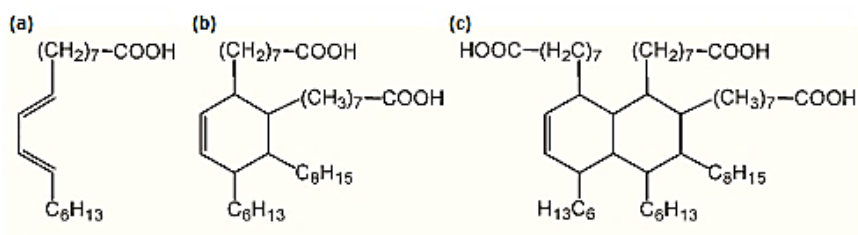
Figure 33: Composition of Pripol 1017: (a) mono-acid, (b) di-acid, (c) tri-acid [3]

Both reagents were added in a 500 ml three-neck flask fitted with a magnetic stirring system, a reflux condenser, an absorber system for water and a nitrogen inlet, as shown in Figure 34. After that, the turbid mixture was heated to 120°C for 2 hours by using a hot oil bath to obtain a transparent blend. Finally, the temperature was increased to 160°C for 24 hours under identical reaction conditions.
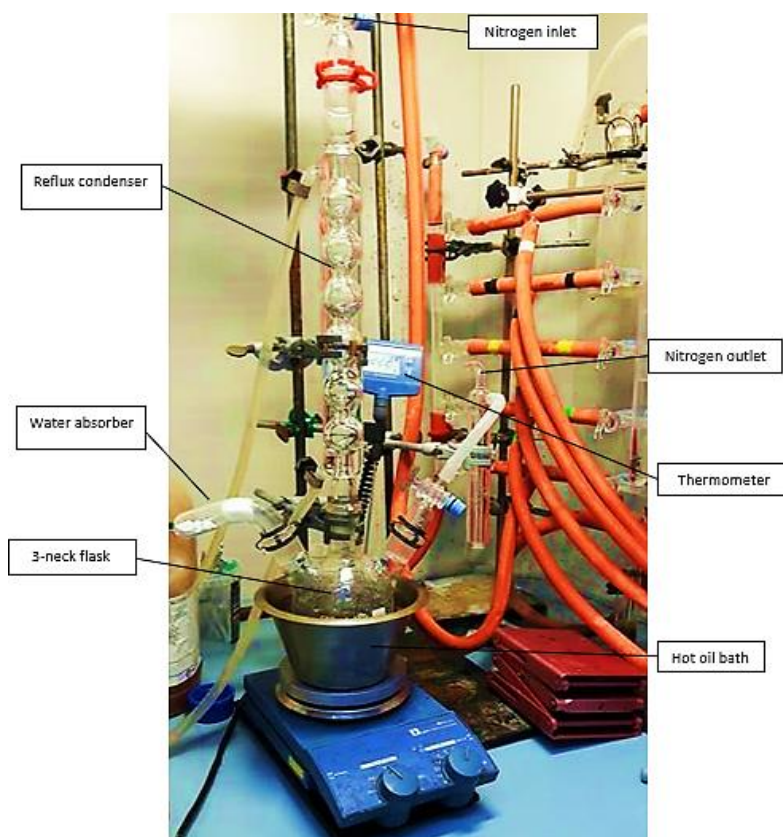
Figure 34: Setup for condensation polymerisation of dipropylene triamine with Pripol 1017

During this synthesis, the carboxyl groups of the fatty acids react with the amine groups of DPTA to form randomly branched oligomers and water. The reaction scheme of this synthesis step is shown in Figure 35.
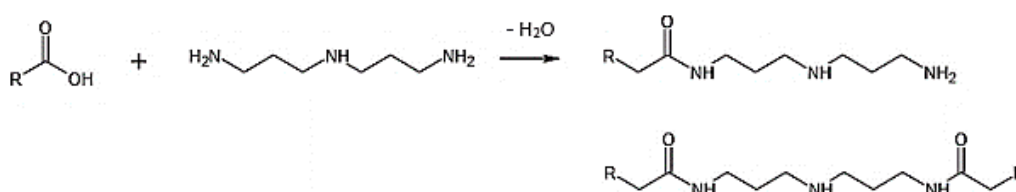
Figure 35: Condensation polymerisation of DPTA with a carboxylic acid

5.1.2 Purification of randomly branched oligomers

The obtained mixture of oligomers was cooled down to room temperature, solubilized in 50 ml of chloroform and put in an ultrasonic bath to dissolve it. Afterwards, 24 ml of methanol and 60 ml of water were mixed into the blend to create two different layers. In the bottom of the flask, a mixture of chloroform and oligomers was obtained. On top of it, a layer of water, methanol and unreacted DPTA was formed. The bottom layer was decanted and the mixture of oligomers and chloroform was purified by repeating this procedure 5 more times. Finally, the chloroform was removed from the mixture to acquire pure oligomers. For this step, a

rotary evaporator was used at the highest vacuum as possible, resulting in a very viscous mixture of randomly branched oligomers.

5.1.3 Condensation of urea with randomly branched oligomers

In the second synthesis step, 20.32 g of the randomly branched oligomers was added into a 250 ml 3-neck flask, fitted with a reflux condenser, nitrogen inlet and stirring system (Figure 36). Afterwards, the 3-neck flask with oligomers was heated in a hot oil bath to 130°C (under a nitrogen atmosphere) while mixing the blend.
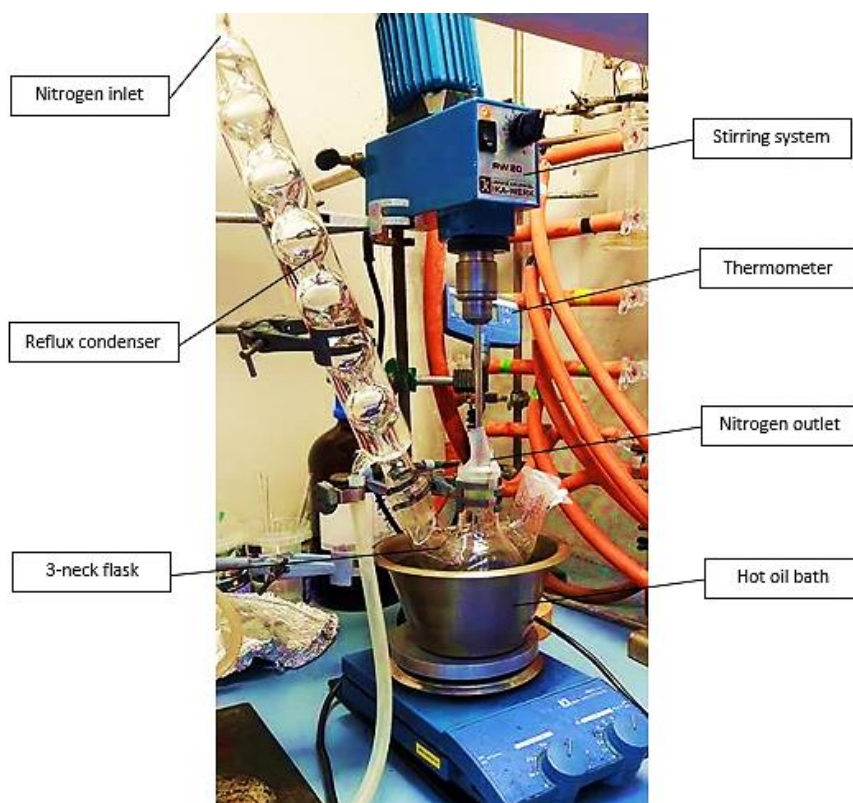
Figure 36: Setup for condensation of urea with randomly branched oligomers

When the temperature was 130°C, 2.68 g solid urea (Mallinckrodt Baker, Inc.) was added to the mixture of oligomers and it reacted for 2 hours at this temperature. Then, the temperature was risen to 140°C by 5°C increments every 60 min. Finally, a very viscous self-healing polymer was created and it was quickly removed while it was hot and elastic [47].

During this synthesis step, the amine groups of the randomly branched oligomers react with the amide groups of urea to form a self-healing mixture. The reaction scheme of this synthesis step is shown in Figure 37.
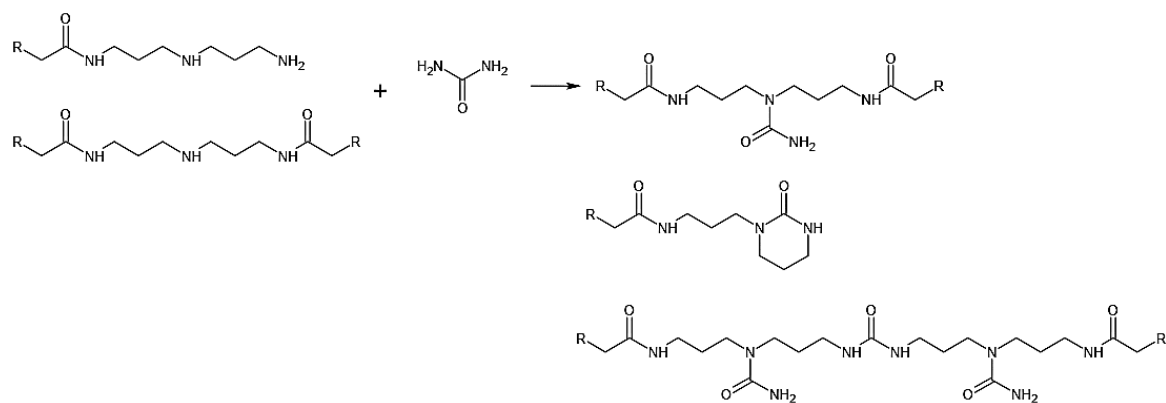
Figure 37: Condensation of randomly branched oligomers with urea

5.2 Synthesis of conductive self-healing elastomer

The formation of cracks can be prevented by using a self-healing elastomeric matrix instead of a traditional elastomer (e.g. polydimethylsiloxane). Although the silver coated copper flakes were preferred from the percolation experiment as 'best' conductive fillers, it was decided to blend the mixture of carbon black nanopowder and carbon nanotubes into the synthesized self-healing elastomer due to its cost-price and availability.

5.2.1 Printability of CosPo

The self-healing elastomeric matrix became a very viscous and sticky polymer after cooling to room temperature. Moreover, the addition of conductive fillers into the self-healing matrix resulted in an extra increase of viscosity. Due to both reasons, it was impossible to deposit the conductive self-healing blend by blade coating or screen printing. Ergo, the viscosity of the conductive self-healing elastomeric matrix (ink) should be reduced in order to be processable. This degree of printability was evaluated with the naked eye and for that reason, it was not always unambiguous to judge.

5.2.2 Reduction of viscosity of conductive self-healing elastomer

There are two different opportunities to decrease the viscosity of the conductive self-healing elastomer. On the one hand, an increase of the blend temperature results in the reduction of the viscosity. On the other hand, it can be lowered by dissolving the self-healing elastomer into a suitable solvent. Both methods were tested in this master's thesis and these results are discussed below.

Increase in temperature:

A heating gun warmed up the self-healing elastomeric matrix, resulting in a small reduction of viscosity. Unfortunately, the blend was still too viscous to use as conductive ink in printing techniques. Moreover, a burned smell was observed during the heating process which

58

indicated a degradation of the self-healing elastomer. Ergo, this test showed clearly that a temperature rise is not a suitable solution to decrease the viscosity of the self-healing rubber.

Addition of solvents:

In this experiment, 5 different solvents were tested to dissolve the self-healing elastomer (and reduce the viscosity), namely chloroform, dimethylformamide (DMF), tetrahydrofuran (THF), 2-methyltetrahydrofuran (2-MeTHF) and cyclopentyl methyl ether (CPME).

Initially, each vial was filled with 0.5 g self-healing elastomer, 0.5 ml solvent and a magnetic bar. Afterwards, the vial was set on a magnetic mixer and the blend was mixed for 6 hours. The finally obtained blend was evaluated with the naked eye on the reduction of the viscosity and thus, the degree of printability. These results are shown in Table 18 with the following possibilities: printable (+), not printable (-) and doubtful to print (±).

Table 18: Printability of self-healing elastomer (concentration: 1.0 g/ml)

Solvent	Concentration: 1.0 g/ml
Chloroform	+
DMF	-
THF	±
2-MeTHF	±
CPME	-

At a concentration of 1.0 g/ml, the self-healing elastomer only dissolved sufficiently in chloroform which resulted in a printable blend. Besides, there was still some solvent present in the vial in case of testing DMF and CPME. Both solvents did not reduce the viscosity to acquire a printable ink. Finally, the blends of the self-healing elastomer in THF and 2-MeTHF looked almost printable, but it was still too dry. The addition of 0.5 ml extra solvent could maybe decrease the viscosity, whose results are demonstrated in Table 19. In this case, the blends had a concentration of 0.5 g/ml and were mixed overnight.

Table 19: Printability of self-healing elastomer (concentration: 0.5 g/ml)

Solvent	Concentration: 0.5 g/ml
Chloroform	+
DMF	-
THF	±
2-MeTHF	-
CPME	-

This experiment clearly showed that DMF, 2-MeTHF and CPME were no suitable solvents to dissolve the self-healing elastomer. The obtained blends were too viscous and sticky to print/deposit. Moreover, there was still a certain amount of solvent present in the vial.

In addition, the THF-based blend looked printable, but it was still pretty sticky. In case of chloroform, the viscosity of the self-healing elastomer was strongly reduced to create a printable blend.

From these results, it was decided to dissolve the self-healing elastomer in a certain amount of chloroform. Although the blend was now printable, it involved some dangers. Chloroform is a hazardous solvent with an intoxicating effect and a boiling point at 61°C. Due to this, it is important to provide a good-working ventilation during the deposition - and curing step.

5.2.3 Preparation of conductive self-healing elastomeric ink

In the second synthesis step of the self-healing elastomer, the randomly branched oligomers reacted with urea which resulted in a non-conductive elastomeric matrix [3]. In this master's thesis, conductive fillers were added to the self-healing elastomer to create conductive paths through the self-healing elastomeric matrix.

During the first part of its heating process (when the reaction temperature was still 130°C), 1.8 g of the mixture of carbon black nanopowder and carbon nanotubes was added (in small amounts) to the mixture of randomly branched oligomers and urea. Taking into account the percolation experiments, this filler load would generate a conductive blend. After 2 hours, the temperature was increased to 140°C by 5°C increments every 60 minutes. Finally, a very viscous blend was obtained which stuck on the stirring stick.

The viscosity of the conductive self-healing elastomer was reduced by adding 150 ml of chloroform while mixing the blend. This surplus of chloroform dissolved all the self-healing rubber in order that the conductive fillers were homogenously mixed. Unfortunately, the viscosity decreased too strongly and the blend became liquid. Due to this, the viscosity should be increased again by using a rotary evaporator (set on 300 mPa) to remove a large volume of chloroform. Finally, a good printable blend (with unknown amount of chloroform) was obtained.

6 Deposition of conductive inks

6.1 Deposition methods

Electronic circuits and applications (e.g. solar cells, LEDs …) can be manufactured by printing ink formulations on various substrates. Currently, there are different printing techniques, such as spray coating, screen printing, inkjet printing, lithography, flexography, blade coating… Due to these techniques, it is simpler and more cost-effective to prepare electronics with (new) improved functionalities. In this master's thesis, two techniques are explained in more depth, namely blade coating and screen printing [75].

During the research, the technique of blade coating was handled to print the (conductive) inks of the percolation experiments to obtain equally thick layers. Afterwards, tensile specimens were cut out of these layers to investigate the correlation between the electrical resistance and the extensibility. Finally, the conductive self-healing elastomeric ink was deposited by blade coating to check its printability.

6.1.1 Blade coating

This deposition method is mostly used to apply a coating layer on the surface of a uniform substrate, such as glass or paper. It is a simple technique whereby initially the thickness of the coating layer should be set. Afterwards, a certain volume of coating material is poured onto the substrate. The blade coater spreads the coating material to form an equally thick layer, which finally is cured.

In this master's thesis, the blade coating technique is employed to produce equally thick layers of (self-healing) conductive elastomers on a glass substrate. The used blade coater (shown in Figure 38) is a stainless steel 'mtv universal film applicator Model UA 3000-220' with a setting range of 0 – 3000 microns and a width of 220 mm [76].

Figure 38: mtv universal film applicator Model UA 3000-200' blade coater [76]

6.1.2 Screen printing

Screen printing is a deposition technique that transfers ink or paste onto a substrate. It consists of five prerequisites to guarantee identically reproducible thick films: a printing medium, a mesh screen, a substrate (to print upon), a squeegee and a protected framework.

Figure 39 represents the screen printing process in three simple steps. First of all, the printing medium (e.g. paste, emulsion or ink) is placed onto the mesh screen and is not in contact with the substrate, because that could damage the final print. In the second step, a flexible squeegee forces the printing medium through the mesh apertures to produce the desired print. Finally, the surplus of printing medium is moved back to the start conditions of this deposition method [31].
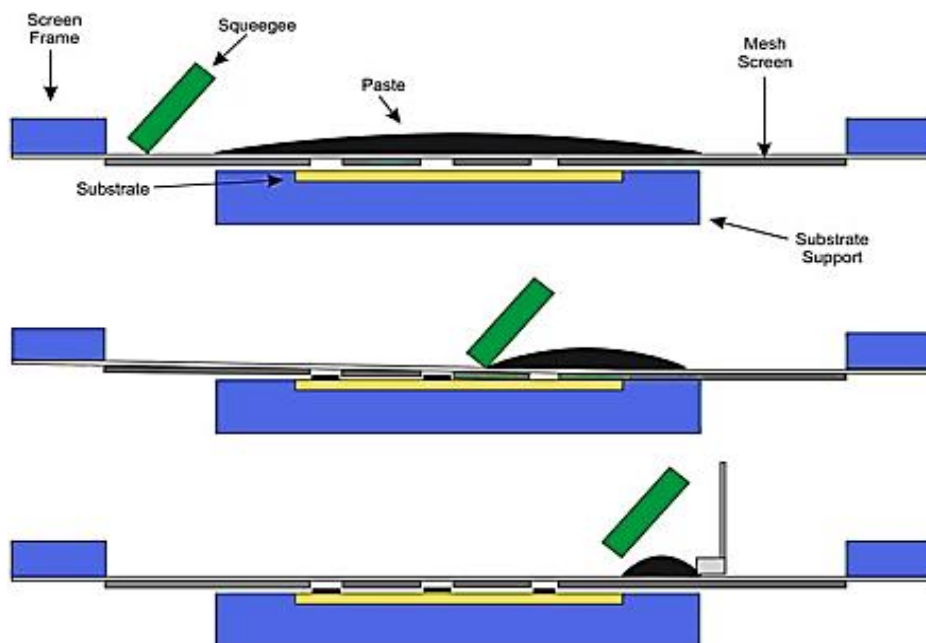
Figure 39: Schematic representation of screen printing process [31]

6.2 Deposition procedure of PDMS-based conductive inks

The PDMS-based conductive inks of all the percolation experiments were separately blade coated to form equally thin layers. Further, conductive specimens were produced from these layers after which the resistance was measured while stretching.

6.2.1 Deposition method of PDMS-based inks

Before blade coating the (conductive) inks of the percolation experiments, a silicone elastomer curing agent (Dow Corning – Sylgard 184) was added in each blend in a 10:1 mass ratio (10 g PDMS – 1 g curing agent). This curing agent formed crosslinks between the polymer chains of PDMS while curing, which resulted in more elasticity and mechanical strength.

Further, each ink was poured onto a glass substrate which was previously injected with a releasing spray (Vosschemie – Trennspray). Due to this injection, it would be easier to remove the coated layer (after curing). Afterwards, a blade coater printed 500 µm thin layers of each ink. Finally, the printed layers were cured for 2 hours in an oven at 120 °C. The finally cured PDMS layers with conductive fillers are demonstrated in Figure 40.
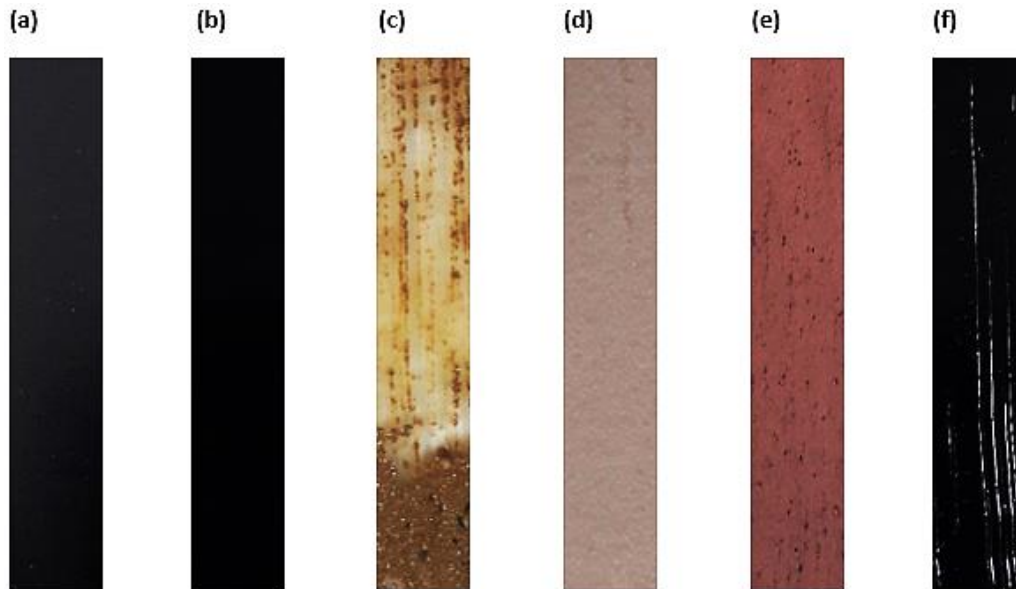
Figure 40: Coated PDMS layers with conductive fillers: (a) carbon black, (b) multi-walled carbon nanotubes, (c) silver nanowires, (d) silver microparticles, (e) silver coated copper flakes and (f) mixture of carbon black and carbon nanotubes

Figure 40 clearly shows that the PDMS-based inks with carbon black (a), multi-walled carbon nanotubes (b) and silver microparticles (d) created uniform well-coated layers. In addition, some particles (conductive fillers) are still visible in the printed layers with the silver coated copper flakes (e) and the mixture of carbon black and carbon nanotubes (f). These inks were not uniformly blended, which resulted in non-smooth layers after blade coating. A possible solution is to heat slightly the blend in order that the particles are mixed more homogenously in the PDMS-matrix. Finally, the printed PDMS layer with silver nanowires (c) did not cure, because there was still too much ethylene glycol present in the ink. Moreover, the silver nanowires agglomerated and for both reasons, this printed layer was a failure. A potential alternative is to disperse the silver nanowires in isopropyl alcohol instead of ethylene glycol, which has a significantly lower boiling point (82.6°C).

Furthermore, some problems were observed during releasing the different layers from the glass substrate. The PDMS layer with carbon black and the PDMS layer with Ag-Cu flakes stuck on the substrate and did not release simply. A big amount of the conductive fillers fell to the bottom (onto the glass substrate) and settled in small solid structures.

This coating step demonstrates that inks with (a big amount of) conductive fillers should be mixed very well and homogenously before printing. Besides, it is interesting to inject a

surplus of releasing spray in order that the gluing of the printed layers to the glass substrate is reduced/prevented.

6.2.2 Fabrication of conductive tensile specimens

This paragraph describes the manufacturing method of (conductive) tensile specimens from the coated layers. Figure 41 shows the design of the specimen with a working length of 25 mm in its narrowed part, a thickness of 500 µm and a width of 10 mm at the edge and 5 mm in the centre.

Figure 41: Design of fabricated specimen

These specimens were cut out of the different (conductive) layers (except the 'layer' with silver nanowires) by using a 'Trotec Speedy 100 R' laser cutter. After that, the excess of the layers was removed to obtain (conductive) stretchable tensile specimens.

6.3 Resistance as a function of extensibility of PDMS-based coated inks

The produced (conductive) specimens were stretched while its resistance was measured to investigate the correlation between both. Due to these measurements, the ultimate elongation of each sample until fracture or loss of conductivity was detected.

6.3.1 Measuring equipment

During this experiment, the (narrowed parts of the) tensile specimens were elongated until fracture with a stretching apparatus. These data were processed and saved in LabVIEW via the operating system, which controlled the stretching apparatus. Meanwhile, the specimen's resistance was measured by using a Keithley 2000 multimeter. The bottom of the tested specimen was in contact with insulating carbon tape, while its top touched a conductive copper tape. This copper tape was connected with the multimeter which sent the measurement results to LabVIEW. Figure 42 shows the whole measuring set-up to determine simultaneously the correlation between the resistance and the elongation.
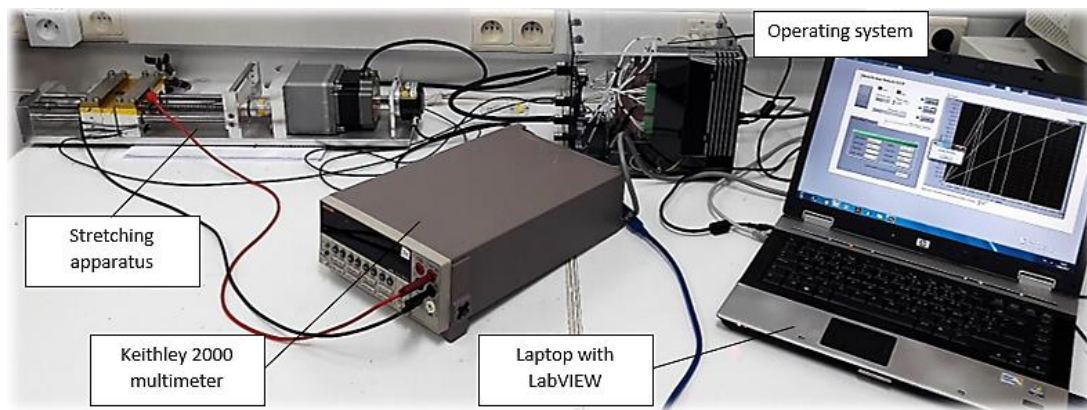
Figure 42: Setup for measuring simultaneously the elongation and the resistance of tensile specimens

6.3.2 Results of tensile tests

The measurement results of the tensile test represent the resistance of the specimen as a function of its elongation. At a certain elongation, the material is no longer conductive and/or the specimen breaks in two pieces. Moreover, it is interesting to observe the correlation between the relative resistance ($\Delta R/R_0$) and the relative elongation ($\Delta L/L_0$). In this case, the variation of the electrical resistance to its original resistance value is examined while stretching the specimen. When the relative resistance remains constant (or decreases) while the elongation increases, the specimen does not lose any conductivity. This phenomenon is required in the formation of stretchable conductors. When the relative resistance increases as a function of the elongation, the material is not suitable to use for stretchable electronic applications. The different fabricated specimens were all tested and these results are discussed below.

PDMS with carbon black:

The tested specimens of PDMS with carbon black were not conductive, because the percolation threshold of the blend was not passed. Due to this, the carbon black particles could not form conductive paths through the matrix which resulted in no electrical conductivity. The rise of the carbon black amount could lead to the formation of these paths, but the blend viscosity did not tolerate it. Besides, the tensile specimens broke at an average relative elongation of 29 mm resulting in a (narrowed) working length of 54 mm. Ergo, the tested specimens (with an extensibility of 116%) were capable to be stretched twice as long as originally. Due to this, the PDMS-specimen with carbon black met the requirement of 100% extensibility.

PDMS with MWCNT's:

The electrical resistance of the two tensile specimens of PDMS with multi-walled carbon nanotubes was dependent on its (relative) elongation, as demonstrated in Figure 43.
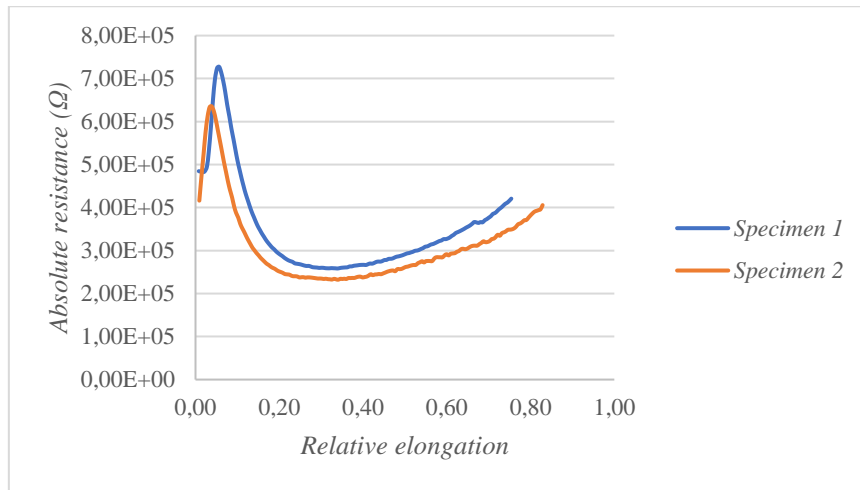
Figure 43: Absolute resistance as a function of relative elongation of PDMS-MWCNT's specimens

Figure 43 shows that the electrical resistance rose at a small elongation, but then it reduced strongly with a further stretch. This decrease was the result of the new position of the cylindrical MWCNT's. Due to stretching the specimen, the conductive fillers oriented in the direction of the elongation which resulted in extra physical entanglement of the multi-walled carbon nanotubes. When the relative elongation amounted approximately 30%, the conductive fillers were teared apart in order that the electrical resistance increased again. Finally, the specimen broke at a relative elongation of 80% while the resistance was still 413 kΩ.

Furthermore, the relative resistance was expressed as a function of the relative elongation, as shown in Figure 44.
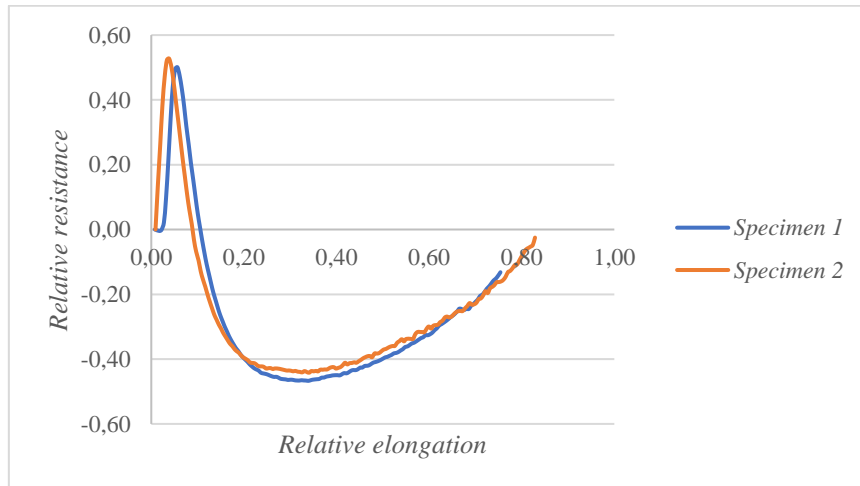
Figure 44: Relative resistance as a function of relative elongation of PDMS-MWCNT's specimens

Figure 44 obviously shows that the PDMS-MWCNT's specimens did not lose any conductivity (compared to the original conductivity) from a relative elongation of 10%, which is very interesting for stretchable conductors. The cylindrical shape of the multi-walled carbon nanotubes caused this positive behaviour, but its conductivity was still too low.

Possible solutions to increase the conductivity are the addition of more conductive fillers or the use of MWCNT's with a lower electrical intrinsic resistance.

PDMS with Ag MP's:

The PDMS samples with silver microparticles did not conduct, because its blend (before curing) was still insulating. In addition, the tensile specimens broke at an average relative elongation of 31%, which is far below the required extensibility of 100%. The large volume percentage of silver microparticles (with a large diameter of 63 µm) obstructed the formation of crosslinks between the PDMS chains while curing. Due to this, the weak specimens had no mechanical strength and broke almost immediately.

PDMS with Ag-Cu flakes:

The PDMS specimens with silver coated copper flakes were stretched while its resistance was measured simultaneously. The correlation between both is demonstrated in Figure 45 by the expression of the relative resistance as a function of the relative elongation.
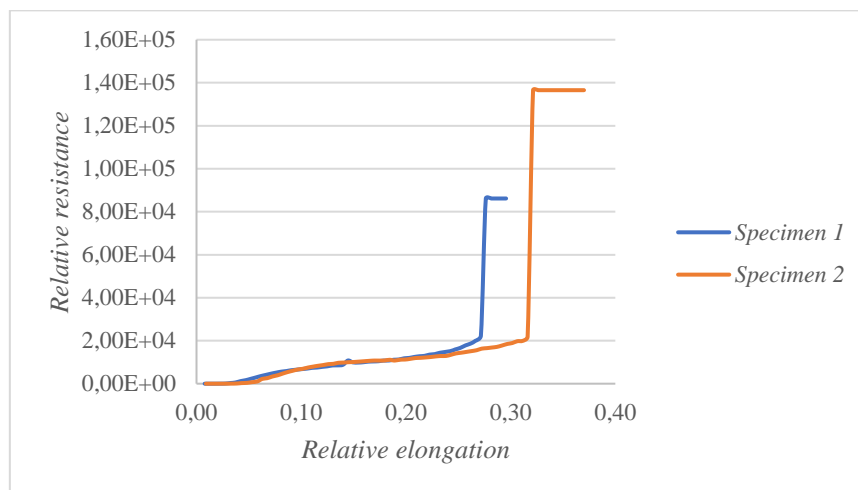
Figure 45: Relative resistance as a function of relative elongation of PDMS specimens with Ag-Cu flakes

The average resistance of the original (not-stretched) specimens amounted 1.14 kΩ, but this value increased strongly while stretching. In addition, both specimens already broke at a relative elongation of 30% and for that reason, it did not meet the requirement of extensibility. Moreover, the final resistance of the samples was ± 25 MΩ which is far too high for electronic applications. Ergo, the cured PDMS layer with silver coated copper flakes did not comply with the requirements of the conductivity (< 1 Ω) and extensibility (100%) so it is not suitable for electronic applications.

PDMS with CB & CNT's:

Two PDMS specimens with the mixture of carbon black nanopowder and carbon nanotubes were tested on its electrical resistance and extensibility. The results of both measurements are represented in Figure 46 by the expression of the relative resistance as a function of the relative elongation.
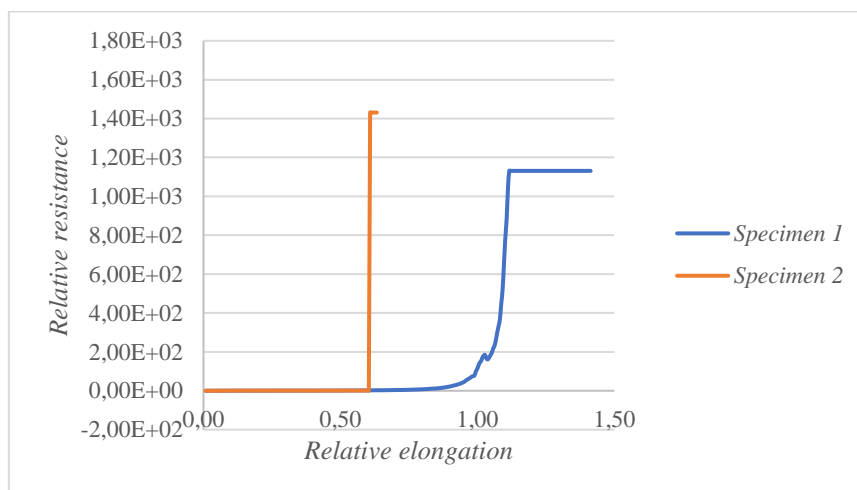
Figure 46: Relative resistance as a function of relative elongation of PDMS specimens with CB & CNT's

Figure 46 obviously shows a big difference between the measurement results of the tested specimens. The first specimen broke at an elongation of 140% while the second specimen already failed at 60%. This failure of the second sample was caused by the presence of a small crack in the specimen before stretching. Due to this observation, the profit of a self-healing elastomer was verified in order that these little cracks are repaired spontaneously without external aid.

Furthermore, the relative resistance of both specimens remained constant until an elongation of 90% (specimen 1) or until fracture (specimen 2) and amounted approximately 95 kΩ, which is still too high then the required 1 Ω for electronic applications.

6.4 Deposition of conductive self-healing elastomeric ink

The conductive self-healing elastomeric ink (dissolved in chloroform) was blade coated to create an equally thin layer with the following properties: flexible, conductive and self-healing.

Initially, the prepared ink was poured onto a glass substrate which was previously injected with a releasing spray (Vosschemie – Trennspray). Afterwards, a blade coater printed two layers with a different thickness, namely 500 µm and 750 µm. Both printed layers were put for 45 minutes on a hot plate (Prazitherm – 2860SR) of 100°C to remove the chloroform. The evaporation of the chloroform caused the formation of some holes, as shown in Figure 47.

Figure 47: Coated self-healing elastomer with mixture of carbon black and carbon nanotubes

Although the self-healing elastomeric ink had an electrical resistance of $\pm$ 30 MΩ (which is still too high for electronic applications), both blade coated layers did not conduct. The formed holes (during the evaporation of chloroform) interrupted the conductive paths through the matrix and caused this non-conductivity.

In addition, the self-healing elastomer usually was a very rigid structure after cooling to room temperature. After a few days/weeks, it became flexible, but this phenomenon did not occur with the coated self-healing elastomer. Both layers remained pretty weak and did not obtain a mechanical strong and flexible texture. A possible explanation is that a certain volume of chloroform was still present in the layer, which could not be released due to the high viscosity of the self-healing elastomer.

7 Conclusion

The overall goal of this master's thesis was to measure in situ the percolation threshold of different conductive fillers in an elastomeric matrix and to integrate them into a self-healing elastomer. In addition, the correlation between the conductivity and extensibility of the coated inks (after curing) was investigated.

A round bottom flask with four built-in tungsten electrodes was used throughout the research to quantify the blend resistance as a function of the conductive filler load. Due to the design of the measuring electrodes, reproducible and accurate results were obtained. Moreover, the cable- and contact resistances were minimised because a four-wire measurement was performed.

Next, the percolation threshold of six different conductive fillers in a PDMS-matrix was determined, namely carbon black (CB), multi-walled carbon nanotubes (MWCNT's), silver nanowires (Ag NW's), silver microparticles (Ag MP's), silver coated copper flakes (Ag-Cu flakes) and a mixture of carbon black nanopowder and carbon nanotubes (CB & CNT's). The finally obtained volume percentage of each conductive filler in a PDMS-matrix and its corresponding blend resistance are represented in Table 20.

Table 20: Finally obtained resistance of each percolation experiment

Conductive filler	Volume percentage (vol%)	Resistance (Ω)
CB	61.16	823097
MWCNT's	6.11	1763
Ag NW's	2.07	No value
Ag MP's	37.50	No value
Ag-Cu flakes	18.14	26.5
CB & CNT's	35.91	73

The percolation experiments obviously show that the percolation threshold of the silver nanowires and the silver microparticles was not passed. Although the percolation threshold of the other conductive fillers was estimated or passed, the blend resistance was still too high for electronic applications. An extra addition of conductive fillers could reduce the blend resistance, but the viscosity did not tolerate it.

Furthermore, the shape of the conductive particles strongly influenced the value of the percolation threshold. Cylindrical particles (e.g. MWCNT's) needed a smaller volume percentage to reach the percolation threshold than spherical particles (e.g. carbon black), because of its higher probability of physical entanglement between the conductive fillers. Besides, the blend resistance of metal fillers was smaller than carbon-based particles, caused by its lower intrinsic electrical resistance.

In addition, the characteristics of the cured PDMS inks with conductive fillers were investigated, especially the correlation between the electrical resistance and the extensibility. This experiment showed that the electrical resistances of PDMS layers with spherical particles (e.g. Ag-Cu flakes) increased while stretching. On the other hand, the conductivity of the layers with cylindrical MWCNT's reduced when increasing its elongation. Unfortunately, the electrical resistance ($\pm$ 413 kΩ) was still too high for electronic applications, but an extra addition of MWCNT's (with a lower intrinsic resistance) can decrease this value.

Finally, the integration of conductive fillers in the self-healing elastomeric matrix resulted in a printable ink by the addition of chloroform. Unfortunately, the chloroform had to be evaporated which caused the formation of small holes. Due to this defect, the coated self-healing elastomeric layer was not conductive. Besides, a certain volume of chloroform was still present in the coated self-healing elastomer, obstructing its flexible properties.

This master's thesis recommends the investigation of some extra topics. First of all, different (more stretchable) silicones should be tested to improve the extensibility of the coated inks. In addition, literature describes several kinds of MWCNT's with a lower intrinsic resistance and a higher aspect ratio. The integration of these conductive fillers can increase the electrical conductivity of a blend, while the percolation threshold decreases. Finally, conductive fillers with a dendrite structure looks promising to reduce the percolation threshold in an elastomeric matrix because of its high probability to form conductive paths.

Bibliography

[1]   T. Lu, L. Finkenauer, J. Wissman and C. Majidi, "Rapid Prototyping for Soft-Matter Electronics," *afm journal,* 2014.

[2]   Y. Wang, Z. Li and J. Xiao, "Stretchable Thin Film Materials: Fabrication, Application, and Mechanics," *Journal of Electronic Packaging,* 2016.

[3]   D. Montarnal, P. Cordier, C. Soulié-Ziakovic, F. Tournilhac and L. Leibler, "Synthesis of Self-Healing Supramolecular Rubbers from Fatty Acid Derivatives, Diethylene Triamine, and Urea," *Journal of Polymer Science: Part A: Polymer Chemistry,* 2008.

[4]   P. Li, K. Sun and J. Ouyang, "Stretchable and Conductive Polymer Films Prepared by Solution Blending," *ACS Applied Materials & Interfaces,* 2015.

[5]   Y.-L. Rao, A. Chortos, R. Pfattner, F. Lissel, Y.-C. Chiu, V. Feig, J. Xu, T. Kurosawa, X. Gu, C. Wang, M. He, J. W. Chung and Z. Bao, "Stretchable Self-Healing Polymeric Dielectrics Cross-Linked Through Metal−Ligand Coordination," *Journal of the American Chemical Society,* 2016.

[6]   J. E. Mates, I. S. Bayer, J. M. Palumbo, P. J. Carroll and C. M. Megaridis, "Extremely stretchable and conductive waterrepellent coatings for low-cost ultra-flexible electronics," *Nature communications,* 2015.

[7]   J. Ruhhammer, M. Zens, F. Goldschmidtboeing, A. Seifert and P. Woias, "Highly elastic conductive polymeric MEMS," *National Institute for Materials Science,* 2015.

[8]   Y. Kim, J. Zhu, B. Yeom, M. Di Prima, X. Su, J.-G. Kim, S. J. Yoo, C. Uher and N. A. Kotov, "Stretchable nanoparticle conductors with self-organized conductive pathways," *Macmillan Publishers,* 2013.

[9]   J. Lee, S. Chung, H. Song, S. Kim and Y. Hong, "Lateral-crack-free, buckled, inkjet-printed silver electrodes on highly pre-stretched elastomeric substrates," *Journal of Physics D: Applied Physics,* 2013.

[10] M. Gonzalez, B. Vandevelde, W. Christiaens, Y.-H. Hsu, F. Iker, F. Bossuyt, J. Vanfleteren, O. Van der Sluis and P. Timmermans, "Design and implementation of flexible and stretchable systems," in *Microelectronics Reliability*, 2011.

[11] K.-S. Kim, K.-H. Jung and S.-B. Jung, "Design and fabrication of screen-printed silver circuits for stretchable electronics," in *Microelectronic engineering*, 2014, pp. 216-220.

[12] S. Hwang and S.-H. Jeong, "Stretchable carbon nanotube conductors and their applications," 2016.

[13] M. Gonzalez, F. Axisa, M. Vanden Bulcke, D. Brosteaux, B. Vandevelde and J. Vanfleteren, "Design of Metal Interconnects for Stretchable Electronic Circuits using Finite Element Analysis".

[14] M. Jablonski, R. Lucchini, F. Bossuyt, T. Vervust, J. Vanfleteren, J. De Vries, P. Vena and M. Gonzalez, "Impact of geometry on stretchable meandered interconnect uniaxial

tensile extension fatigue reliability," in *Microelectronics Reliability*, 2015, pp. 143-154.

[15] Y. Hou, D. Wang, X.-M. Zhang, H. Zhao, J.-W. Zha and Z.-M. Dang, "Positive piezoresistive behavior of electrically conductive alkyl-functionalized graphene/polydimethylsilicone nanocomposites," *Journal of Materials Chemistry C,* 2013.

[16] G. A. Gelves, B. Lin, U. Sundararaj and J. A. Haber, "Low Electrical Percolation Threshold of Silver and Copper Nanowires in Polystyrene Composites," *Advanced Functional Materials,* pp. 2423-2430, 2006.

[17] M. Park, J. Park and U. Jeong, "Design of conductive composite elastomers for stretchable electronics," *Elsevier,* 2014.

[18] Elveflow: Plug & Play Microfluidics, "Introduction about PDMS soft-lithography and polymer molding for microfluidics," 2015. [Online]. Available: http://www.elveflow.com/microfluidic-tutorials/soft-lithography-reviews-and-tutorials/introduction-in-soft-lithography/introduction-about-soft-lithography-and-polymer-molding-for-microfluidic/.

[19] C.-C. Chang, Z.-X. Huang and R.-J. Yang, "Three-dimensional hydrodynamic focusing in two-layer polydimethylsiloxane (PDMS) microchannels," in *Journal of Micromechanics and Microengineering*, 2007, pp. 1479-1486.

[20] G.-W. Huang, H.-M. Xiao and S.-Y. Fu, "Wearable Electronics of Silver-Nanowire/Poly(dimethylsiloxane) Nanocomposite for Smart Clothing," *Scientific reports,* 2015.

[21] F. Xu and Y. Zhu, "Highly Conductive and Stretchable Silver Nanowire Conductors," in *Advanced Materials*, 2012, pp. 5117-5122.

[22] X. Wang, T. Li, J. Adams and J. Yang, "Transparent, stretchable, carbon-nanotube-inlaid conductors enabled by standard replication technology for capacitive pressure, strain and touch sensors," *Journal of Materials Chemistry A,* 2013.

[23] Z. Yu, X. Niu, Z. Liu and Q. Pei, "Intrinsically Stretchable Polymer Light-Emitting Devices Using Carbon Nanotube-Polymer Composite Electrodes," *Advanced Materials,* 2011.

[24] H. Denver, T. Heiman, E. Martin, A. Gupta and D.-A. Borca-Tasciuc, "Fabrication of polydimethylsiloxane composites with nickel nanoparticle and nanowire fillers and study of their mechanical and magnetic properties," *Journal of Applied Physics,* 2009.

[25] S. Shang, W. Zeng and X.-m. Tao, "High stretchable MWNTs/polyurethane conductive nanocomposites," *Journal of Materials Chemistry,* 2011.

[26] M. G. Urdaneta, R. Delille and E. Smela, "Stretchable Electrodes with High Conductivity and Photo-Patternability," *Advanced Materials,* 2007.

[27] A. Goyal, A. Kumar, P. K. Patra, S. Mahendra, S. Tabatabaei, P. J. J. Alvarez, G. John and P. M. Ajayan, "In situ Synthesis of Metal Nanoparticle Embedded Free Standing Multifunctional PDMS Films," in *Macromolecular Rapid Communications*, 2009, pp. 1116-1122.

74

[28] P. J. Brigandi, J. M. Cogen and R. A. Pearson, "Electrically Conductive Multiphase Polymer Blend Carbon-Based Composites," *Polymer Engineering and Science,* 2014.

[29] M. Kontopoulou, M. Kaufman and A. Docoslis, "Electrorheological properties of PDMS/carbon black suspensions under shear flow," *Springer,* 2009.

[30] M. Sumita, K. Sakata, S. Asai, K. Miyasaka and H. Nakagawa, "Dispersion of fillers and the electrical conductivity of polymer blends filled with carbon black," *Polymer Bulletin,* 1991.

[31] C. W. Foster, R. O. Kadara and C. E. Banks, Screen-Printing Elektrochemical Architectures, Springer, 2016.

[32] J. Essam, "Percolation theory," in *Reports on Progress in Physics*, 1980, pp. 835-840.

[33] J. E. Steif, A mini course on percolation theory, 2009, p. 2009.

[34] Wolfram MathWorld, "Percolation theory," 23 March 2017. [Online]. Available: http://mathworld.wolfram.com/PercolationTheory.html.

[35] I. Mutlay and L. B. Tudoran, "Percolation Behavior of Electrically Conductive Graphene Nanoplatelets/Polymer Nanocomposites: Theory and Experiment," in *Fullerenes, Nanotubes, and Carbon Nanostructures*, 2014, pp. 413-433.

[36] S. Kim, S. Choi, E. Oh, J. Byun, H. Kim, B. Lee, S. Lee and Y. Hong, "Revisit to three-dimensional percolation theory: Accurate analysis for highly stretchable conductive composite materials," *Scientific Reports,* 2016.

[37] A. Bunde and W. Dieterich, "Percolation in Composites," *Journal of Electroceramics,* 2000.

[38] R. M. Mutiso, "Electrical Percolation In Metal Nanowire Networks For Bulk Polymer Nanocomposites And Transparent Conductors, And Resistive Switching In Metal/polymer Nano-Gap Devices," 2013.

[39] W.-Z. Cai, S.-T. Tu and J.-M. Gong, "A Physically Based Percolation Model of the Effective Electrical Conductivity of Particle Filled Composites," *Journal of Composite Materials,* 2005.

[40] V. Kumar and A. Rawal, "Tuning the electrical percolation threshold of polymer nanocomposites with rod-like nanofillers," in *Polymer*, Elsevier, 2016.

[41] J. Liang and Q. Yang, "Aggregate structure and percolation behavior in polymer/carbon black conductive composites," *Journal of Applied Physics,* 2007.

[42] Cancarb, "Physical & Chemical Properties of Carbon Black," 2016.

[43] S. P. Lacour, "Stretchable Thin-Film Electronics," in *Stretchable Electronics*, Wiley-VCH Verlag GmbH & Co. KGaA, 2013, pp. 81-109.

[44] M. Adler, R. Bieringer, T. Schauber and J. Günther, "Materials for Stretchable Electronics Compliant with Printed Circuit Board Fabrication," in *Stretchable electronics*, Wiley-VCH Verlag GmbH & Co. KGaA., 2013, pp. 161-185.

[45] A. Mata, A. J. Fleischman and S. Roy, "Characterization of Polydimethylsiloxane (PDMS) Properties for Biomedical Micro/Nanosystems," in *Biomedical microdevices*, Springer Science + Business Media, 2005, pp. 281-293.

[46] Dow Corning, *Product Information Sylgard 184 Silicone Elastomer,* 2014.

[47] C. Wang, H. Wu, Z. Chen, M. T. McDowell, Y. Cui and Z. Bao, "Self-healing chemistry enables the stable operation of silicon microparticle anodes for high-energy lithium-ion batteries," *Nature Chemistry,* pp. 1042-1048, 2013.

[48] K. Guo, D.-L. Zhang, X.-M. Zhang, J. Zhang, L.-S. Ding, B.-J. Li and S. Zhang, "Conductive Elastomers with Autonomic Self-Healing Properties," *Polymer Chemistry,* p. 12127–12133, 2015.

[49] Q. Wu, J. Wei, B. Xu, X. Liu, H. Wang, W. Wang, Q. Wang and W. Liu, "A robust, highly stretchable supramolecular polymer conductive hydrogel with self-healability and thermo-processability," *Nature,* 2016.

[50] Encyclopaedia Britannica , "Carbon Black," 2017.

[51] Mitsubishi Chemical, "Manufacturing Process of Carbon Black," [Online]. Available: http://www.carbonblack.jp/en/cb/seizou.html. [Accessed 11 April 2017].

[52] J. Yang and J. Liang, "A modified model of electrical conductionfor carbon black–polymer composites," *Society of Chemical Industry,* pp. 738-742, 2010.

[53] W. Li, Z.-Y. Liu and M.-B. Yang, "Preparation of Carbon Black/PolypropyleneNanocomposite with Low Percolation Threshold UsingMild Blending Method," *Journal of Applied Polymer Science,* 2008.

[54] Intelligent Materials , "Multi Walled Carbon Nano Tube MWCNT," [Online]. Available: http://www.nanoshel.in/multi-walled-carbon-nano-tube.html. [Accessed 13 April 2017].

[55] AzoNano, "Multiwall Carbon Nanotubes (MWCNT): Production, Analysis and Application," 24 May 2013. [Online]. Available: http://www.azonano.com/article.aspx?ArticleID=3469. [Accessed 13 April 2017].

[56] J. Zhang, M. Mine, D. Zhu and M. Matsuo, "Electrical and dielectric behaviors and their origins in the three-dimensional polyvinyl alcohol/MWCNT composites with low percolation threshold," in *Carbon*, 2009, pp. 1311-1320.

[57] J.-B. Lee and D.-Y. Khang, "Electrical and mechanical characterization of stretchable multi-walled carbon nanotubes/polydimethylsiloxane elastomeric composite conductors," *Composites Science and Technology,* p. 1257–1263, 2012.

[58] S. Maiti, S. Suin, N. K. Shrivastava and B. B. Khatua, "Low Percolation Threshold in Polycarbonate/Multiwalled CarbonNanotubes Nanocomposites Through Melt Blending withPoly(butylene terephthalate)," *Journal of Applied Polymer Science,* pp. 543-553, 2013.

[59] A. Khosla and B. L. Gray, "Preparation, characterization and micromolding of multi-walled carbon nanotube polydimethylsiloxane conducting nanocomposite polymer," in *Materials Letters*, 2009, p. 1203–1206.

[60] I. Singh, A. Verma, I. Kaur, L. M. Bharadwaj, V. Bhatia, V. K. Jain, C. S. Bhatia, P. K. Bhatnagar and P. C. Mathur, "The Effect of Length of Single-Walled Carbon

Nanotubes (SWNTs) on Electrical Properties of Conducting Polymer-SWNT Composites," *Journal of Polymer Science,* pp. 89-95, 2009.

[61] X. Liang, T. Zhao, Y. Hu and R. Sun, "Dielectric properties of silver nanowires-filled polyvinylidene fluoride composite with low percolation threshold," *Journal of Nanoparticle Research,* 2014.

[62] A. Lonjon, P. Demont, E. Dantras and C. Lacabanne, "Low filled conductive P(VDF-TrFE) composites: Influence of silver particles aspect ratio on percolation threshold from spheres to nanowires," *Journal of Non-Crystalline Solids,* pp. 3074-3078, 2012.

[63] Metallpulver24, "Silberpulver," 2017. [Online]. Available: https://www.metallpulver24.de/de/silberpulver-1g-grundpreis-eur-1400-kg.html. [Accessed 12 April 2017].

[64] M. Zulkarnain, A. B. Muhamad Husaini, M. Mariatti and I. A. Azid, "Particle Dispersion Model for Predicting the Percolation Threshold of Nano-Silver Composite," *Arabian Journal for Science and Engineering,* p. 2363–2376, 2016.

[65] Metallpulver24, "Kupferpulver eConduct," [Online]. Available: https://www.metallpulver24.de/de/kupferpulver-econduct-50g-dose.html. [Accessed 11 April 2017].

[66] H.-S. Chuang and S. Werely, "Design, fabrication and characterization of a conducting PDMS for microheaters and temperature sensors," *Journal of Micromechanics and Microengineering,* 2009.

[67] S. Jan, S. T. Buschhorn and K. Schulte, "Comparison of rheological and electrical percolation phenomena in carbon black and carbon nanotube filled epoxy polymers," *Journal of Materials Science,* pp. 659-669, 2011.

[68] US Research Nanomaterials, "Super Conductive Carbon Black Nanopowder and Carbon Nanotube Mixed," [Online]. Available: http://www.us-nano.com/inc/sdetail/4509. [Accessed 11 April 2017].

[69] J. Hong, D. W. Park and S. E. Shim, "Electrical, Thermal, and Rheological Properties of Carbon Black and Carbon Nanotube Dual Filler-Incorporated Poly(dimethylsiloxane) Nanocomposites," *Macromolecular Research,* pp. 465-472, 2011.

[70] Keithley Instruments, "Two-Wire vs. Four-Wire Resistance Measurements: Which Configuration Makes sense for Your Application?," 2013.

[71] US Research Nanomaterials, "Super Adsorption Activated Porous Carbon Powder," [Online]. Available: http://www.us-nano.com/inc/sdetail/32769. [Accessed 11 April 2017].

[72] Sigma-Aldrich, "Carbon nanotube, multi-walled," 2017. [Online]. Available: http://www.sigmaaldrich.com/catalog/product/aldrich/659258?lang=en&region=BE. [Accessed 13 April 2017].

[73] RAS AG , *Technical Information ECOS - silver nanowire technology,* 2016.

[74] B. C.-K. Tee, C. Wang, R. Allen and Z. Bao, "An electrically and mechanically self-healing composite with pressure- and flexion-sensitive properties for electronic skin applications," *Nature Nanotechnology,* pp. 825-832, 2012.

[75] IMO-IMOMEC, "Printable electronics," [Online]. Available: https://www.uhasselt.be/UH/IMO/Research-domains/Printable-electronics.html. [Accessed 1 June 2017].

[76] mtv messtechnik, "mtv universal film applicator Model UA 3000-220," 2017. [Online]. Available: http://webshop.mtv-messtechnik.de/epages/mtvwebshop.sf/en_US/?ObjectPath=/Shops/mtvwebshop/Products/MTUA3000-220. [Accessed 15 April 2017].

Auteursrechtelijke overeenkomst

Ik/wij verlenen het wereldwijde auteursrecht voor de ingediende eindverhandeling:
In Situ Measurement of Percolation Threshold of Conductive Fillers and Integration into a Self-Healing Elastomer

Richting: **master in de industriële wetenschappen: chemie**
Jaar: **2017**

in alle mogelijke mediaformaten, - bestaande en in de toekomst te ontwikkelen - , aan de Universiteit Hasselt.

Niet tegenstaand deze toekenning van het auteursrecht aan de Universiteit Hasselt behoud ik als auteur het recht om de eindverhandeling, - in zijn geheel of gedeeltelijk -, vrij te reproduceren, (her)publiceren of distribueren zonder de toelating te moeten verkrijgen van de Universiteit Hasselt.

Ik bevestig dat de eindverhandeling mijn origineel werk is, en dat ik het recht heb om de rechten te verlenen die in deze overeenkomst worden beschreven. Ik verklaar tevens dat de eindverhandeling, naar mijn weten, het auteursrecht van anderen niet overtreedt.

Ik verklaar tevens dat ik voor het materiaal in de eindverhandeling dat beschermd wordt door het auteursrecht, de nodige toelatingen heb verkregen zodat ik deze ook aan de Universiteit Hasselt kan overdragen en dat dit duidelijk in de tekst en inhoud van de eindverhandeling werd genotificeerd.

Universiteit Hasselt zal mij als auteur(s) van de eindverhandeling identificeren en zal geen wijzigingen aanbrengen aan de eindverhandeling, uitgezonderd deze toegelaten door deze overeenkomst.

Voor akkoord,

Machiels, Jarne

Datum: **12/06/2017**